Simulation of Seasonal and Interhemispheric Variations in the Stratospheric Circulation

SYUKURO MANABE AND J. D. MAHLMAN

Geophysical Fluid Dynamics Laboratory/NOAA, Princeton University, Princeton, N. J. 08540

(Manuscript received 10 December 1975, in revised form 7 July 1976)

ABSTRACT

This paper describes the stratosphere as simulated by the time integration of a global model of the atmosphere as developed at the Geophysical Fluid Dynamics Laboratory of NOAA.

It is shown that the model is capable of simulating a number of the features of the seasonal variation in the stratosphere. For example, it qualitatively reproduces the seasonal reversals of zonal wind direction in the mid-stratosphere between westerlies in winter and the zonal easterlies prevailing during the summer season. In the mid-latitude region of the lower model stratosphere, zonal mean temperature is highest in the winter when solar radiation is weak. At the cold equatorial tropopause of the model, the seasonal variation of temperature is also quite different from that which would be expected from the seasonal variation of solar radiation. These results are in qualitative agreement with the observed variation.

Attempts are made to identify the factors which are responsible for the various aspects of the seasonal variation of the model stratosphere, based upon detailed budget analyses of angular momentum, heat and eddy kinetic energy. It is found that, with the exception of the high-latitude regions, the seasonal variation of temperature in the lower model stratosphere is essentially controlled by dynamical effects rather than by the seasonal variation of local heating due to solar radiation.

The stratosphere as simulated by the global model has large interhemispheric asymmetries in the shape of the polar westerly vortex, the magnitudes and the distributions of eddy kinetic energy, and the meridional circulation in the winter hemisphere. Interhemispheric asymmetries in orography are apparently responsible for the interhemispheric differences in the quasi-stationary component of energy flux from the troposphere to the stratosphere of the model, and thus account for many of the asymmetries in the stratospheric circulation. In particular, the simulated stratospheric Aleutian anticyclone is shown to be related to the presence of the strong quasi-stationary tropospheric jet stream off the east coast of Asia.

Some of the important shortcomings of the model in simulating the stratosphere include an exaggeration of the magnitudes of the various components of the eddy kinetic energy budget at the top computational level (10 mb) of the model and an overestimation of the intensity of the polar westerly vortex. Also, the model fails to reproduce the mid-winter "sudden stratospheric warming" phenomenon and the quasi-biennial wind reversal in the equatorial stratosphere. It is suggested that the performance of the model at the top level suffers from the coarseness in the vertical finite-difference resolution and the lid boundary condition imposed at the top of the model atmosphere.

1. Introduction

Many attempts have been made to simulate the general circulation of the joint stratosphere-troposphere system during the past 10 years. For example, Smagorinsky *et al.* (1965) and Manabe *et al.* (1965) tried to reproduce the thermal and dynamical structure of the stratosphere by use of a hemispheric general circulation model in which the explicit radiative and dynamical processes are allowed to freely interact with each other. On the other hand, Peng (1965) made a similar attempt using a simple quasi-geostrophic spectral model in which the vertical distribution of mean static stability is prescribed, and the fields of prognostic variables are represented by a limited number of spherical harmonics. It is encouraging that both models successfully simulate the latitudinal variation of temperature in the lower stratosphere. Manabe and Hunt (1968) refined the model of Smagorinsky *et al.* by increasing the vertical computational resolution. They demonstrated that their model is capable of simulating many of the observed features such as the sharp equatorial tropopause, the tropopause gap, and the latitudinal variation of the height of the tropopause. Furthermore, the energetics of the circulation in their model stratosphere is in qualitative agreement with the energetics in the actual stratosphere as obtained by Oort (1964).

The studies mentioned above did not include the effects of non-zonal forcing, such as those of mountains and land-sea contrast. This was done by many authors, i.e., Bryon-Scott (1967), Clark (1970), Holloway and Manabe (1971), Miyakoda *et al.* (1970), Matsuno (1970, 1971), Trenberth (1973), Kasahara *et al.* (1973), Manabe and Terpstra (1974) and Kasahara and

Sasamori (1974). For example, Miyakoda showed that his hemispheric model with realistic orography is capable of forecasting the splitting of the polar vortex in winter. Bryon-Scott, Matsuno and Trenberth found that their non-zonal models produce a phenomenon which resembles the so-called "sudden stratospheric warmings." Matsuno discussed how non-zonal forcing can cause such a drastic change in the model stratosphere. Kasahara *et al.* and Manabe and Terpstra showed that their models are capable of simulating the general shape of the planetary waves and demonstrate the dominating effects of mountains in maintaining quasi-stationary planetary waves in the model stratosphere.

As is known, the stratospheric circulation changes markedly from winter to summer and from one hemisphere to another (e.g., Labitzke and van Loon, 1972). Unfortunately, one of the common features of the studies mentioned above is that they deal mostly with the dynamics of the stratosphere in one season or one hemisphere. Recently, Cunnold *et al.* (1975) constructed a spectral model with fixed static stability by employing the quasi-geostrophic approximation. Their model includes the effect of seasonal variation as well as a global computational domain. However, it prescribes the topographical distribution of the Northern Hemisphere in both hemispheres for the sake of computational efficiency. Therefore, their model cannot contain any interhemispheric asymmetries induced by orographic differences.

In this study an attempt is made to simulate the seasonal variation and the interhemispheric asymmetries in the stratospheric circulation. By modifying the model constructed by Holloway and Manabe (1971), a global model of the joint stratosphere-troposphere system has been constructed in which the seasonal variations of sea surface temperature, ozone and solar radiation are taken into consideration. This study contains a detailed description of the seasonal variation of the thermal and dynamical structure of the model stratosphere. It identifies some of the successes and failures in simulating various features of the stratosphere. Furthermore, attempts are made to determine some of the important dynamical factors which control the seasonal variations and the interhemispheric asymmetries in the structure of the model stratosphere. In a companion study, properties of the circulation in the model stratosphere are further explored by performing numerical experiments on the dispersion of inert tracers (e.g., Mahlman, 1973a). One of the goals of the present study, together with the tracer studies, is to help provide a comprehensive picture of how the stratospheric circulation transports quantities such as momentum, heat, energy and inert tracers.

Some other aspects of this seasonal model have been described in preceding publications. For example, Hayashi (1974) discussed the dynamical structure of the large-scale disturbances in the tropics of this model. His paper explains how these disturbances transport heat and momentum in the model tropics and is therefore relevant to the present study. See also Manabe *et al.* (1974) and Hahn and Manabe (1975) for further discussions of the general circulation in the model tropics. Detailed descriptions of the climatology and the hydrology of this model are contained in the paper by Manabe and Holloway (1975). Some preliminary aspects of the stratosphere of this model were presented in Mahlman and Manabe (1972).

2. Brief description of the model

The global model used for this study is a modified version of the model of Holloway and Manabe (1971). Also, it is described in Manabe and Holloway (1975) and Manabe *et al.* (1974). One of the main differences of this model from the earlier version is that it undergoes seasonal variation.

The model incorporates the primitive equations of motion in a spherical coordinate system. The numerical problems associated with the treatment of mountains are reduced by using the "sigma" system in which pressure, normalized by surface pressure, is the vertical coordinate (Phillips, 1957). It is assumed that vertical sigma-velocity is equal to zero at the top and the bottom of the model atmosphere. This so-called "lid boundary condition" implies that the wave energy reaching the top is reflected without absorption. In order to approximate the effects of subgrid-scale mixing, the nonlinear viscosity suggested by Smagorinsky (1963) is employed. The finite-difference forms of the dynamical equations are similar to those proposed by Kurihara and Holloway (1967). Their global grid system is modified such that the horizontal grid size of approximately 265 km is as uniform as possible (see Fig. 2.2 of Manabe *et al.*, 1974). In the vertical direction, 11 finite-difference levels are chosen so that the model can crudely simulate the structure of the stratosphere as well as that of the planetary boundary layer. The standard pressures and approximate heights of these 11 levels can be seen in Table 1 of Manabe *et al.* (1974) and in Fig. 3.1.

The scheme for computing radiative heating and cooling is identical with that described by Manabe and Strickler (1964) and Manabe and Wetherald (1967). The solar radiation at the top of the atmosphere is a function of latitude and season. Diurnal variation is eliminated for the sake of simplicity and computational efficiency. The seasonal variation of insolation is controlled by changes in both the declination of the sun and its distance. An annual mean observed distribution of clouds, which varies with latitude and height but not with longitude, is used in the computation of radiative transfer. Three atmospheric gases are also taken into consideration for the computation of radiative

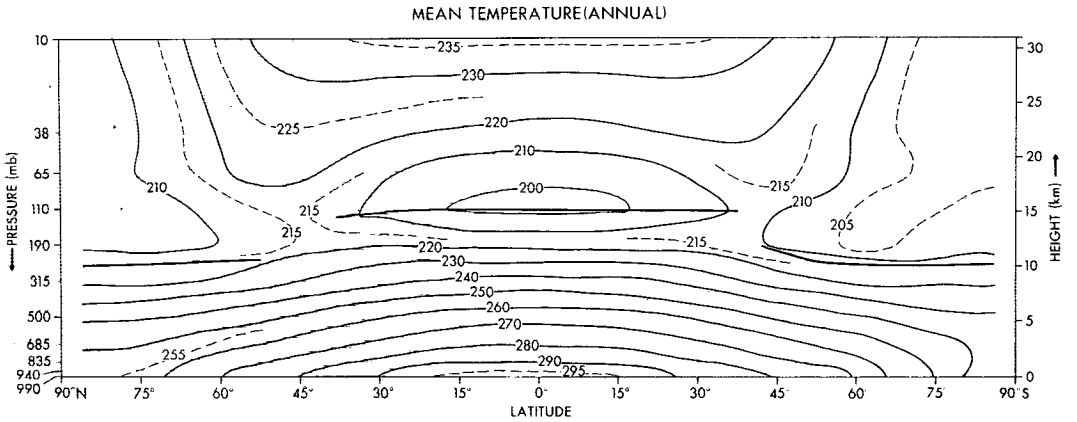

FIG. 3.1. Latitude-height distribution of annual, zonal mean temperature (K) in the model atmosphere.

transfer: water vapor, carbon dioxide and ozone. The distribution of water vapor is computed by a prognostic system which will be described later. The mixing ratio of carbon dioxide is assumed to have a constant value of 0.456×10^{-3} everywhere. The ozone mixing ratio is not a prognostic variable, but is prescribed as a function of latitude, height and season according to the data of Hering and Borden (1964). It is assumed that the distribution of ozone in the Southern Hemisphere is a mirror image of the values employed for the analogous season in the Northern Hemisphere.

The surface temperature over land is determined by the boundary condition that no heat be stored in the ground, i.e., net fluxes of solar and terrestial radiation and the turbulent fluxes of sensible and latent heat all locally add to zero. Over the oceanic part of the model, a seasonal variation of surface temperature is prescribed. It is determined by interpolating in time between observed distributions of monthly mean sea surface temperatures for the months of February, May, August and November. Data from the *World Atlas of Sea Surface Temperatures* [revised by the Hydrographic Office (1944)] are used for this purpose.

The prognostic system of water vapor consists of the contributions by three-dimensional advection of water vapor, evaporation from the earth's surface, vertical mixing of water vapor in the planetary boundary layer, nonconvective condensation and the so-called "moist convective adjustment." For details of the moist convective adjustment scheme, see Manabe *et al.* (1965).

The schemes for computing the hydrology of the ground surface are similar to those described by Manabe (1969). The rates of change of soil moisture and snow depth are determined by the budget of water, snow and heat at the ground surface.

The numerical time integration of the model is continued for a period of approximately 3.5 model years. The initial condition for this integration is obtained from the study of Holloway and Manabe (1971). It is the mean state attained by the long-term integration of a global model which had January insolation and sea surface temperatures as imposed boundary conditions. The first 1.5 model years are time integrated on a grid with low horizontal resolution (~530 km). A high-resolution (~265 km) grid is used for time integrating the final two model years. Results from the time integration of the final model year are analyzed for this study.[1] The various annual mean quantities shown represent averages for the last model year. For the purpose of computing the declination and distance of the sun this 3.5-year period is considered to begin in February 1962.

3. Zonal mean temperature

In Fig. 3.1 the distribution of the annual mean temperature in the model atmosphere is shown as a function of latitude and height. According to this figure, the height of the equatorial tropopause is significantly higher than that of the polar tropopause. In the subtropics of the model the so-called tropopause gap exists between these two tropopauses. At the 110 mb level (i.e., the level of the equatorial tropopause), temperature is lowest around the equator and increases with increasing latitude up to middle latitudes, where it is at a maximum. In general, the temperature at this level is colder in lower latitudes than in higher latitudes. At the 10 mb level, the latitudinal temperature

[1] Examination of the annual march of various quantities indicates that they do not repeat themselves closely from one year to another. This results from a code error in the program of subgrid-scale mixing which was found and corrected at the beginning of the final year of the time integration. The nature of the error was such that momentum rather than relative angular velocity is mixed by the subgrid mixing. Thus, the mixing contributes to the net generation of relative angular momentum over the entire domain. In more specific terms, it removes comparatively small relative angular momentum from the stratospheric jet in high latitudes and adds large relative angular momentum in low latitudes. This code error caused an excessive intensification of stratospheric westerlies at the 10 mb level. The removal of this error is mainly responsible for the interannual variation mentioned above. Its effects on the zonal currents in the model troposphere and lower stratosphere are very small.

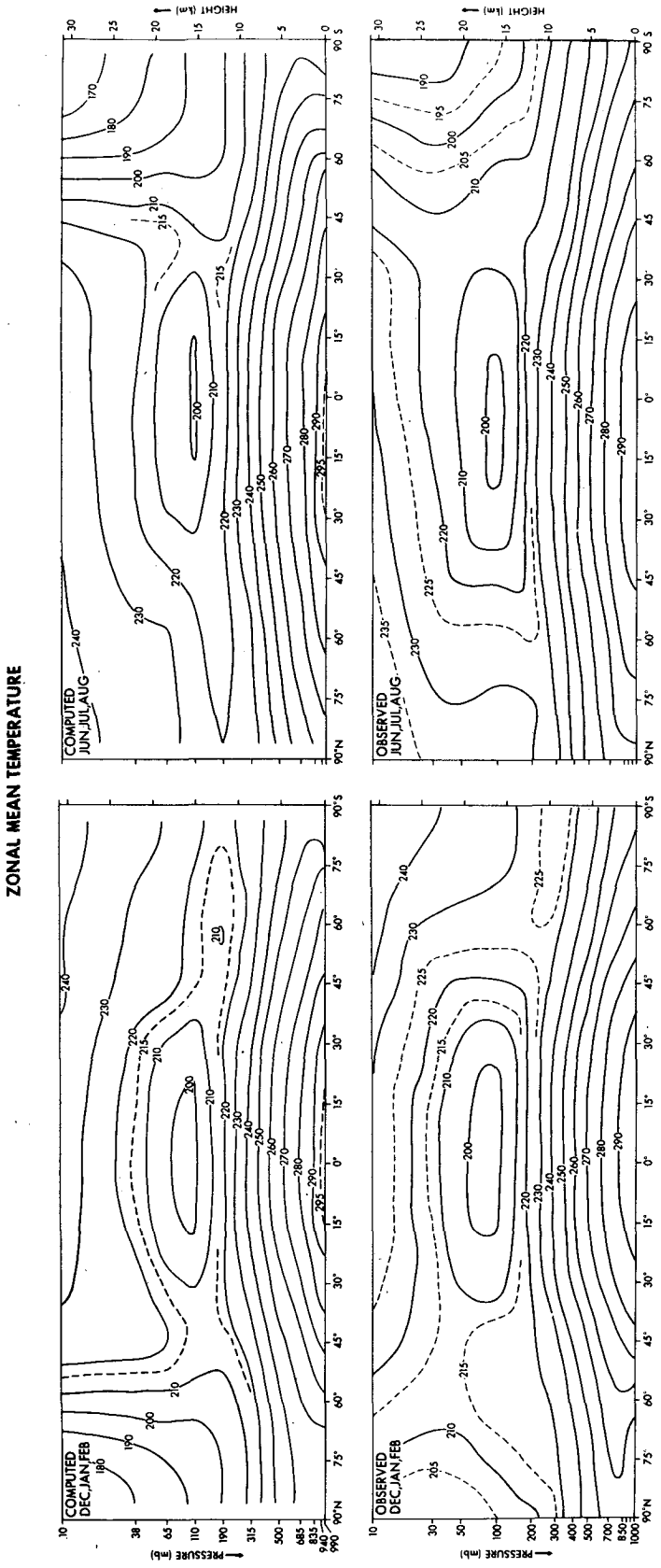

FIG. 3.2. Latitude-height distributions of zonal mean temperature (K). Left: December–February; right: June–August; top: computed distribution; bottom: observed distribution. (Data source: Newell *et al.*, 1969.)

gradient reverses so that temperature is warmest in low latitudes and coldest near the poles. The annual mean features of the model stratosphere described above are in reasonable agreement with those in the actual stratosphere. An essentially similar distribution of zonal mean temperature was obtained by Smagorinsky *et al.* (1965) and Manabe and Hunt (1968) using models with annual mean insolation.

The seasonal variation of the thermal structure of the model atmosphere is illustrated in Fig. 3.2 which shows the latitude-height distribution of zonal mean temperature during the periods December–February and June–August. For the sake of comparison, the corresponding distributions in the actual atmosphere are added to the same figure by using data from Newell *et al.* (1969).

During winter the temperature in the lower stratosphere of the model increases poleward up to middle latitudes, but decreases sharply toward the pole. On the other hand, the latitudinal increase continues all the way to the pole in summer. In the polar regions the temperature as well as its vertical gradient undergoes large seasonal variations. In winter the temperature of the polar stratosphere decreases with increasing altitude throughout the model stratosphere, whereas in summer it increases very gradually with increasing altitude. In low latitudes the inversion is maintained throughout the year and the amplitude of the seasonal variation of temperature is relatively small. Careful inspection of Fig. 3.2, however, reveals that the temperature of the equatorial tropopause is slightly warmer in July than in January. The features of the seasonal variation of the thermal structure of the model stratosphere described above are in basic agreement with those in the actual stratosphere.

There are, however, some important differences between the observed and computed temperature. In particular, the temperature of the model polar stratosphere is too cold by more than 20 K during the polar night. This is a most important difficulty encountered in the simulation of the stratosphere. The basic causes for this unrealistic feature have yet to be conclusively identified, but appear to be mainly attributable to the use of the "lid" upper boundary condition and the poor vertical resolution near the top model level.

In order to examine the seasonal variation of the temperature in the lower stratosphere of the model, the latitude-time distribution of the temperature deviation from the annual mean at 110 mb is shown in Fig. 3.3. For the sake of comparison, the corresponding distribution at 100 mb in the actual atmosphere is added to the same figure. According to this figure, the amplitude of the seasonal variation of temperature in the lower stratosphere is at a maximum in the polar region, in qualitative agreement with the features of the actual atmosphere. However, the amplitude is too large by approximately a factor of 2. This is consistent

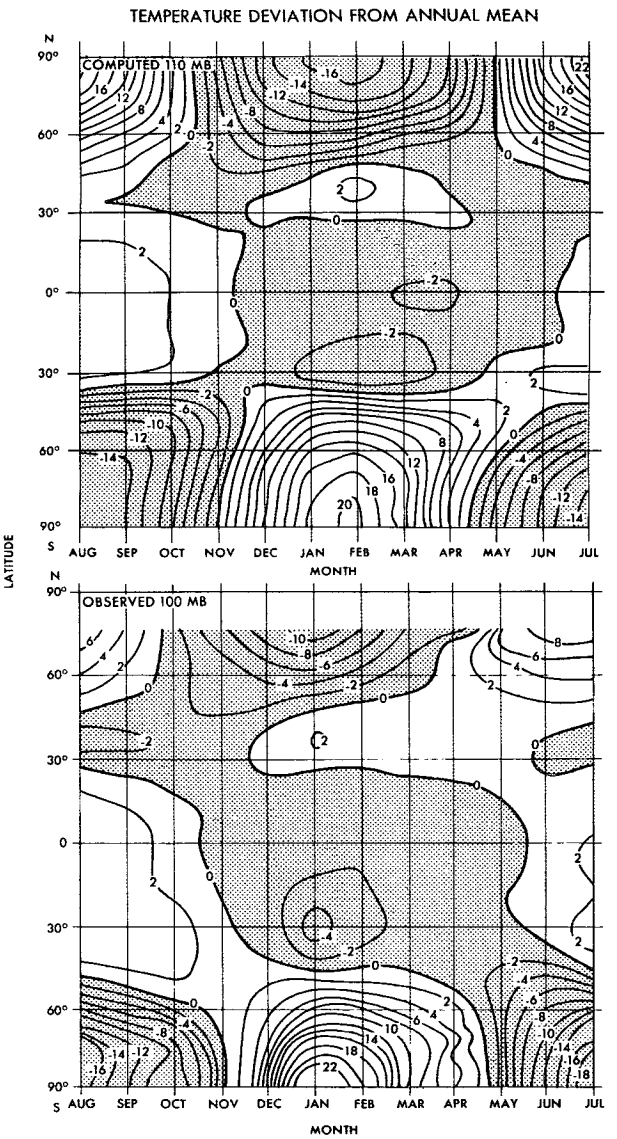

FIG. 3.3. Latitude-time distribution of the deviation of zonal mean temperature (K) from the simulated annual mean value. Top: computed distribution at 110 mb; bottom: observed distribution at 100 mb. (Data sources: Oort and Rasmussen, 1971; Taljaad *et al.*, 1969.)

with the unrealistically cold winter polar temperatures mentioned earlier. In middle latitudes, temperature is at a maximum in winter when the intensity of solar radiation is weakest. Similar features are evident in the observed distribution. In the model tropics the magnitude of seasonal variation in the lower stratosphere is relatively small. It is noteworthy, however, that the temperature is lower during the period December–May and higher during the period June–September. This feature is well illustrated in Fig. 3.4, which shows the height-time distribution of temperature deviation from the annual mean at the model equator. The corresponding observed distribution at the actual equator is also

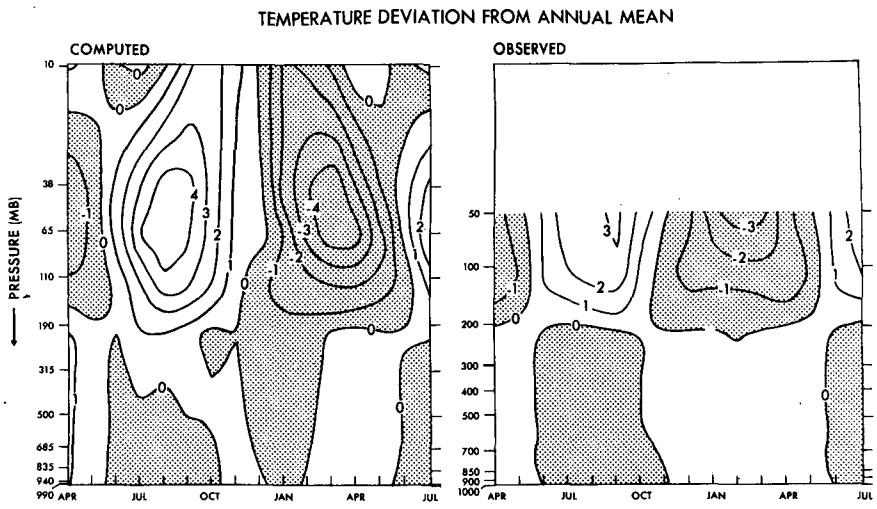

FIG. 3.4. Time-height distribution of the deviation of zonal mean temperature (K) from annual mean value at the equator. Left: computed distribution; right: observed distribution (Oort and Rasmussen, 1971).

added to the same figure for comparison. According to this figure, the phase and the amplitude of stratospheric temperature variation at the model equator approximately agree with those of the actual tropics. A detailed discussion of the implications of this result is given in Section 8 of this paper.

4. Zonal wind

In Fig. 4.1 the latitude-height distributions of zonal wind in the model atmosphere are compared with those in the actual atmosphere.[2] Some of the most important stratospheric phenomena are the reversals of the direction of zonal wind between winter westerlies and summer easterlies. It is encouraging that the model simulates these phenomena. However, the intensity of the polar night jet in the model stratosphere is too strong by a factor of 2. This discrepancy in high latitudes of the winter hemisphere is consistent with the unrealistically large meridional temperature gradient in the model stratosphere mentioned in the preceding section. Fig. 4.1 also indicates that the polar night jet in the model stratosphere is located at somewhat too low a latitude. Also, the separation of the polar jet in the stratosphere and the subtropical jet in the upper troposphere is not sufficient.

The seasonal variation of zonal wind in the model stratosphere is illustrated by Fig. 4.2, which shows the latitude-time distribution of zonal wind at the 10 mb level with a comparison against observation. According to this comparison, the summertime easterlies are generally too weak and do not last long enough as compared with the observed easterlies. It is encouraging, however, that the model simulates successfully the seasonal variation of the easterly jet in low latitudes. As Fig. 4.2 indicates, the core of the easterly jet moves from one summer hemisphere to the other with the passage of seasons. For further discussion of this subject, see Section 7.

5. Meridional circulation

Fig. 5.1 shows the latitude-height distribution of streamfunction of the meridional circulation in the model atmosphere during four months of the year.[3] In both January and July an extensive but weak meridional circulation cell occupies the stratosphere of the summer hemisphere and extends up to the mid-latitudes of the winter hemisphere. This cell accounts for the weak equatorward flow during the first half of the summer season and helps maintain the easterlies (see Section 7 for further discussion of this subject). In higher latitudes of the winter hemisphere an apparent extension of the so-called tropospheric Ferrel cell predominates in the model stratosphere. This is in agreement with results from analyses of the actual stratosphere (e.g., Miyakoda, 1963). This cell is very pronounced during the winter of the Northern Hemisphere and exhibits upward motion in high latitudes and downward motion in middle latitudes. This is in marked contrast to the Southern Hemisphere stratosphere where a much weaker and less extensive three-cell meridional circulation is evident with mean descent in the south polar region. In view of the pronounced two-cell

[2] It should be pointed out that the observed zonal flow in the equatorial stratosphere is obtained by averaging over the easterly and westerly phases of the quasi-biennial oscillation. In this experiment, the westerly phase is not successfully simulated.

[3] During the course of this analysis, it was found that the usual sampling of the wind data once a day is not sufficient for obtaining a representative distribution of the time-averaged mean meridional circulation in the model atmosphere. As pointed out by Hunt and Manabe (1968), a model atmosphere often contains zonally symmetric inertial gravity waves with periods of approximately 11.5 h. In order to avoid the sampling error caused by this oscillation, the wind data of every time step are used for the computation of the results shown in Fig. 5.1.

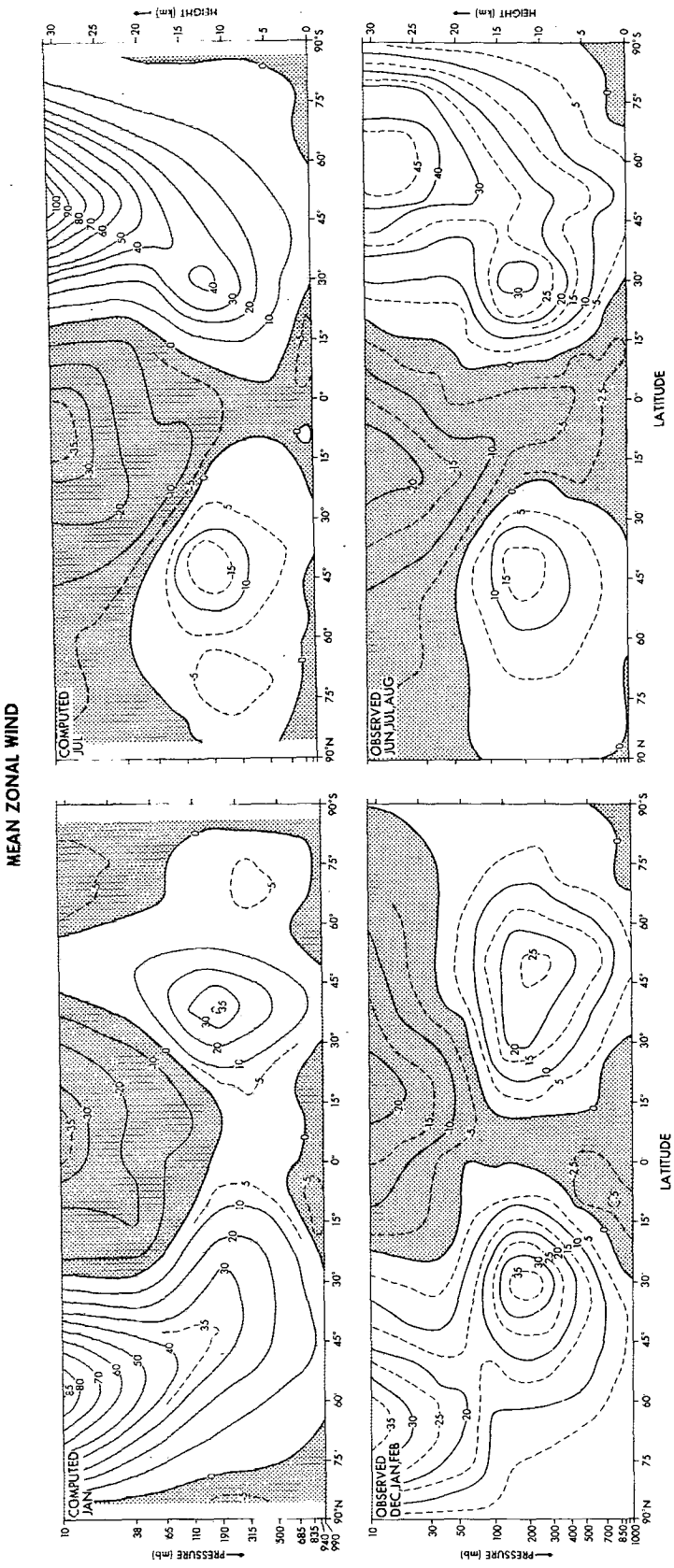

FIG. 4.1. Latitude-height distributions of monthly mean zonal wind (m s^{-1}). Top: computed distributions in January (left) and July (right); bottom: observed distribution in December–February period (left) and June–August period (right). (Data source: Newell *et al.*, 1969.)

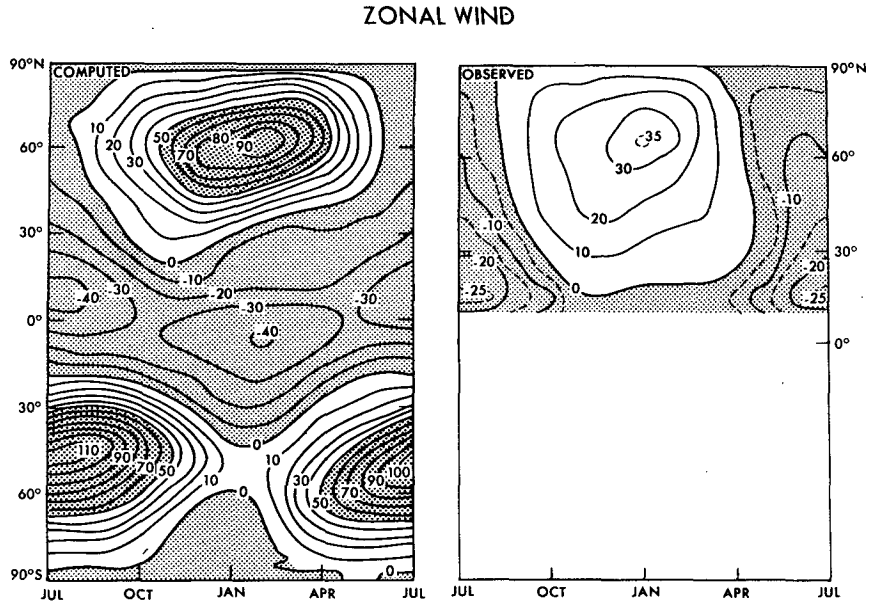

FIG. 4.2. Latitude-time distribution of zonal mean wind (m s^{-1}) at 10 mb. Top: computed distribution; bottom: observed distribution. (Data source: Richards, 1967.)

pattern in the Northern Hemisphere stratosphere, this is a surprising result. There is recent evidence of its presence in the actual atmosphere by inference from heat balance requirements as calculated from satellite-measured temperatures (Adler, 1973; Hartmann, 1975). An observational study by Mahlman (1969a) showed that the Northern Hemisphere meridional circulation can also exhibit a three-cell structure in cases where the usually pronounced waves become weak and the flow becomes essentially zonal (more like the usual state of the Southern Hemisphere stratosphere).

The simulated contrast in the intensity and structure of meridional circulation thus suggests a significant difference between the stratospheric circulations of the two hemispheres. Also large interhemispheric asymmetries are evident in other sections of this paper, as well as in the companion tracer experiments (Mahlman, 1973a) and wave analyses (Hayashi, 1974) based on the results of this simulation experiment.

6. Eddy kinetic energy

The distribution of eddy kinetic energy in the model stratosphere undergoes a large seasonal variation. This is evident in Fig. 6.1, which shows latitude-height distributions of eddy kinetic energy averaged over two quarterly periods—December–February and June–August. The observed distributions for these two periods are added to the same figure for the sake of comparison [data from Oort and Rasmusson (1971) and Richards (1967)]. This figure indicates that during the period December–February, the eddy kinetic energy in the model stratosphere is particularly large in higher latitudes of the Northern Hemisphere. The stratospheric maximum in the distribution of eddy kinetic energy is separated from the tropospheric maximum by a belt of minimum eddy kinetic energy in the lower stratosphere. As the season progresses from winter to summer, the eddy kinetic energy in the model stratosphere decreases by a factor of 50 or more. In the Southern Hemisphere, eddy kinetic energy undergoes a qualitatively similar seasonal variation, except that its magnitude during winter is significantly smaller than that of the Northern Hemisphere. Again, the eddy kinetic energy is very small during the summer season. Comparison of Figs. 6.1 and 4.1 shows that the eddy kinetic energy is particularly small in the latitude-height domain where the zonal wind is easterly. As pointed out by Eliassen and Palm (1960), Charney and Drazin (1961) and Charney (1969), the boundary between easterlies and westerlies should tend to inhibit the propagation of quasi-stationary components of energy flux from source regions. This may provide part of the reason why the stratospheric eddy kinetic energy is particularly small in the summer hemisphere and in equatorial regions where zonal flows are easterly.

The distribution of eddy kinetic energy discussed above may be compared with the corresponding distributions in the actual atmosphere shown in Fig. 6.1. This comparison indicates that the latitude of maximum eddy kinetic energy in the model stratosphere tends to be too low during the winter season. However, the general features of the distribution seem to be in good qualitative agreement with those of the actual stratosphere.

One of the most significant characteristics shown in Fig. 6.1 is that the model eddy kinetic energy in the winter stratosphere of the Northern Hemisphere is much larger than the corresponding quantity in the

Southern Hemisphere. Using results from numerical experiments with general circulation models, Kasahara *et al.* (1973) and Manabe and Terpstra (1974) have shown that the large-scale mountain ranges, such as the Tibetan Plateau and Rocky Mountains, may be chiefly responsible for maintaining the quasi-stationary planetary waves in the winter stratosphere. Based upon results from a theoretical study, Charney and Drazin (1961) concluded that very long waves penetrate into the stratosphere much more easily than short waves,

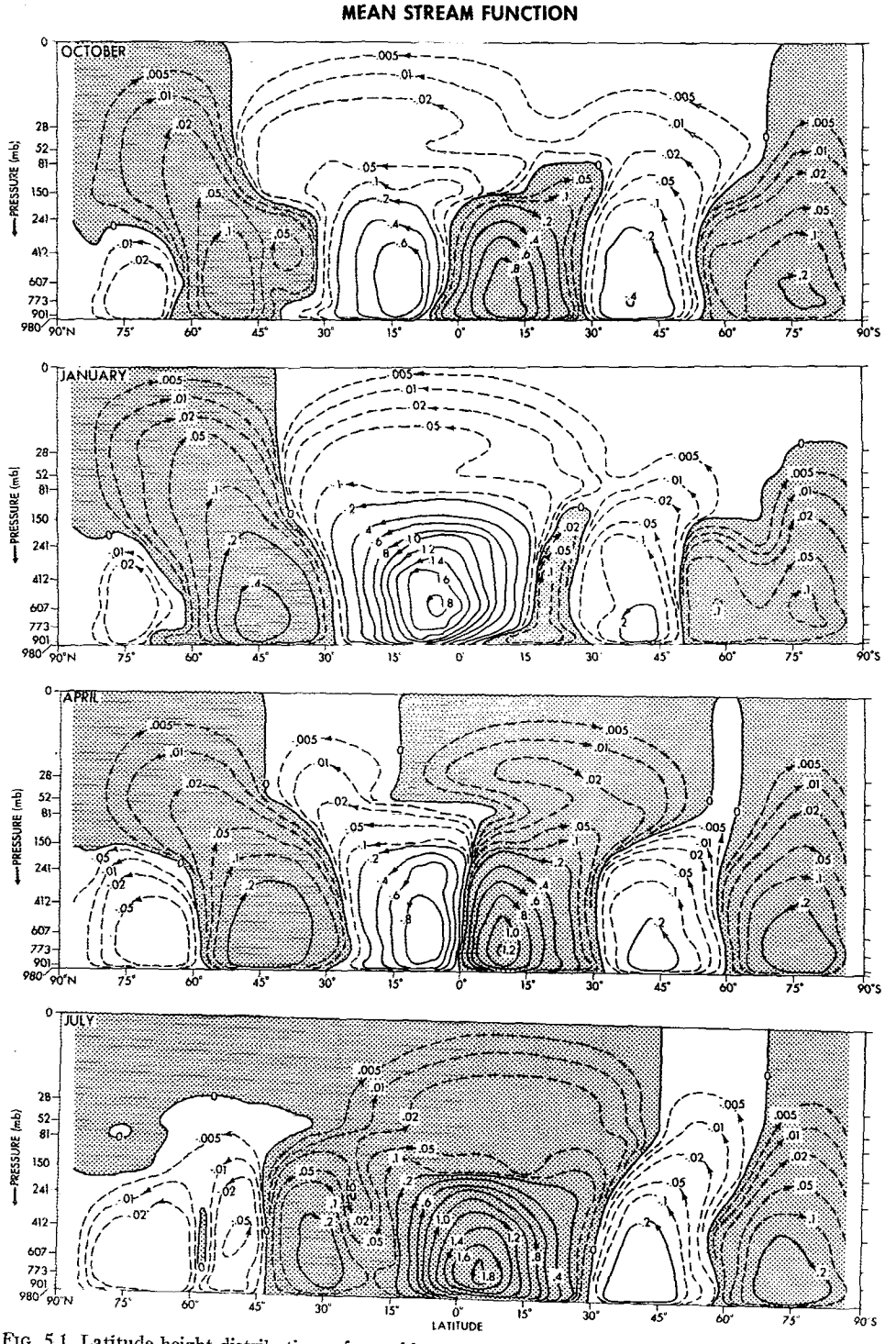

FIG. 5.1. Latitude-height distributions of monthly mean streamfunction (10^{11} kg s^{-1}) of the meridional circulation in the model atmosphere during January, April, July and October.

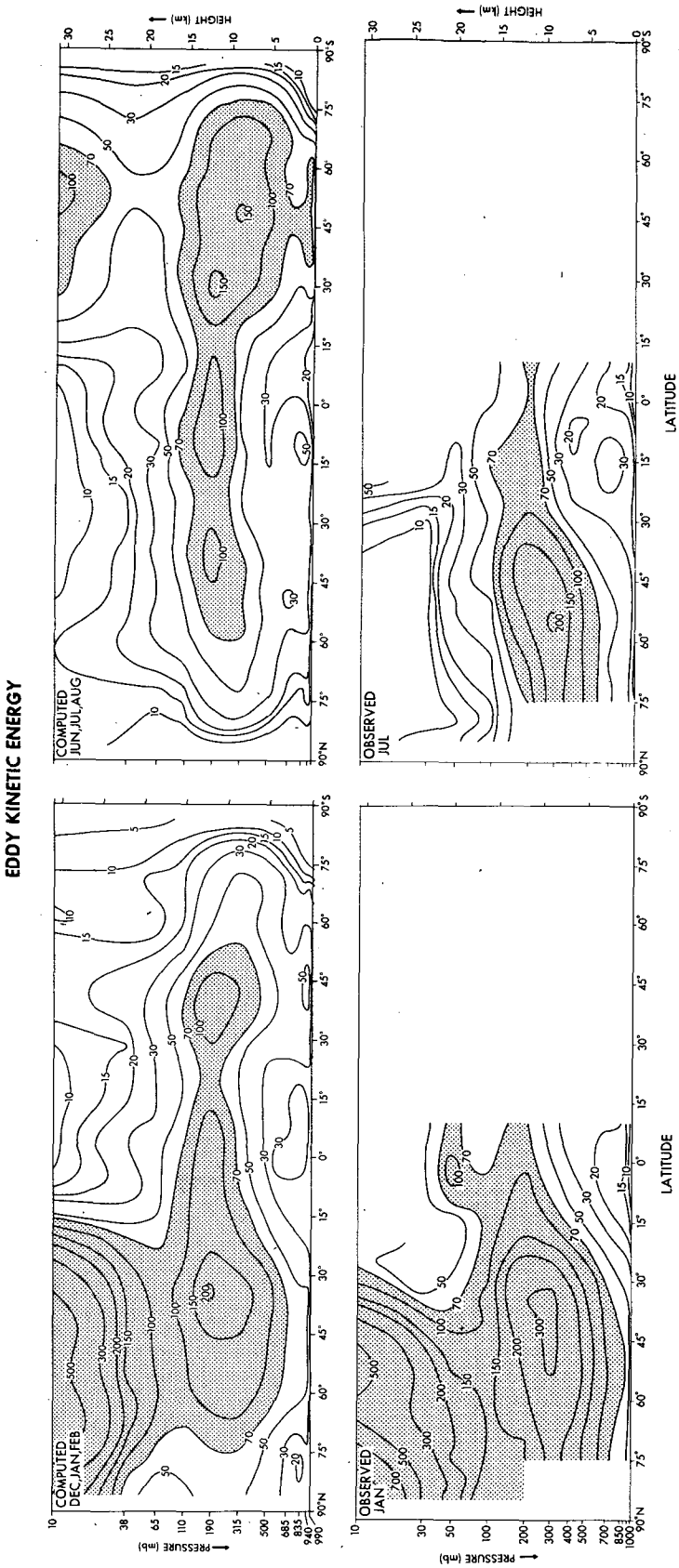

FIG. 6.1. Latitude-height distributions of mean eddy kinetic energy (J kg^{-1}). Top: computed distribution in December–February period (left) and June–August period (right); bottom: observed distribution in January (left) and July (right). (Data sources: Oort and Rasmussen, 1971; Richards, 1967.)

except during summer when easterlies occupy the stratosphere and prevent upward penetration of the energy flux at almost all wavelengths. Therefore, it is probable that interhemispheric differences in the topography of the earth's surface are mainly responsible for the interhemispheric difference in the magnitude of eddy kinetic energy in the model stratosphere.

It is useful to subdivide eddy kinetic energy into the following two components, i.e., kinetic energy of stationary eddies k_E^{ST} and of transient eddies k_E^{TR}. These are defined by

$$k_E^{ST}=\tfrac{1}{2}[(\bar{u}^t-\overrightarrow{\bar{u}^t}^{\lambda})^2+(\bar{v}-\overrightarrow{\bar{v}^t}^{\lambda})^2], \tag{6.1}$$

$$k_E^{TR}=\tfrac{1}{2}[((u-\bar{u}^t)-\overrightarrow{(u-\bar{u}^t)}^{\lambda})^2 + ((v-\bar{v}^t)-\overrightarrow{(v-\bar{v}^t)}^{\lambda})^2], \tag{6.2}$$

where u and v denote the zonal and meridional component of wind, and the t and λ superscripts indicate one-month mean and zonal-mean operators, respectively. In Fig. 6.2 the 10 mb latitude-time distributions of these two components in the model atmosphere are compared. This figure shows that the partition of eddy kinetic energy into stationary and transient components during the winter half of the year is quite different from one hemisphere to another. In the Northern Hemisphere, the stationary component accounts for the major part of eddy kinetic energy, whereas in the Southern Hemisphere, it is somewhat less than the transient component. As discussed above, major mountain systems such as the Rocky Mountain Range and Tibetan Plateau are probably responsible for the predominance of the quasi-stationary disturbances in the Northern Hemisphere stratosphere.

7. Angular momentum budget

Starting with this section, a number of zonal mean balances of various quantities will be presented. Thus, it should be pointed out that the zonal mean balances described here contain some discrepancies. The net tendencies of various quantities do not always exactly equal the sum of the terms involved. These imbalances occur due to interpolation error as well as ambiguity in transforming the model vertical velocity from sigma to pressure coordinates (Mahlman and Moxim, 1976). However, in most cases, these imbalances appear to be too small to alter the conclusions presented here.

As described in Section 4, the zonal wind in the model stratosphere completely changes direction from winter to summer at the top finite-difference level (i.e., the 10 mb level), in qualitative agreement with the behavior of the actual atmosphere. However, the results from the top level may suffer from distortions caused by the coarseness in the vertical grid resolution and the "lid" boundary condition adopted for this study. Nevertheless, this level is analyzed so as to gain insight into the

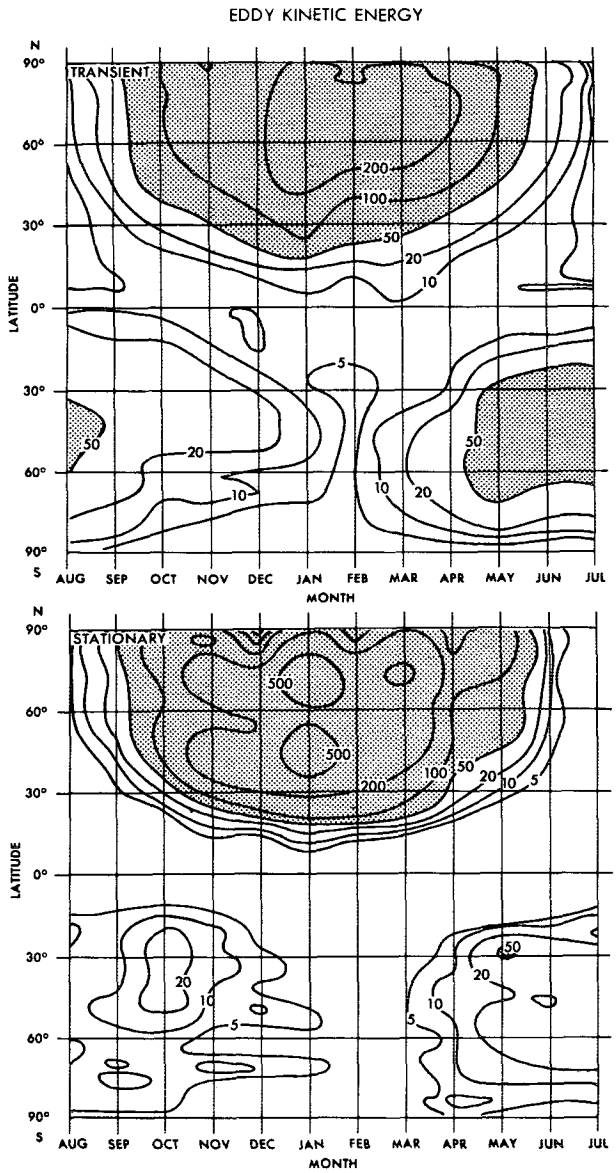

FIG. 6.2. Latitude-time distribution of two components of eddy kinetic energy (J kg^{-1}) at the 10 mb level of the model atmosphere. Top: transient eddy; bottom: standing eddy.

mechanisms responsible for the seasonal reversal of zonal wind direction.

The seasonal variation of the budget of angular momentum in the mid-stratosphere of the model is illustrated in Fig. 7.1 which shows the latitudinal distributions of various components of the budget at the 10 mb level during four typical months of the year. According to this figure, the balance requirement of angular momentum in winter is satisfied by nearly complete compensation between the contributions of large-scale eddies and meridional circulation. Discussion of the possible causes for this compensation follow.

The quasi-geostrophic perturbation analysis of Charney and Drazin (1961) and Dickinson (1969)

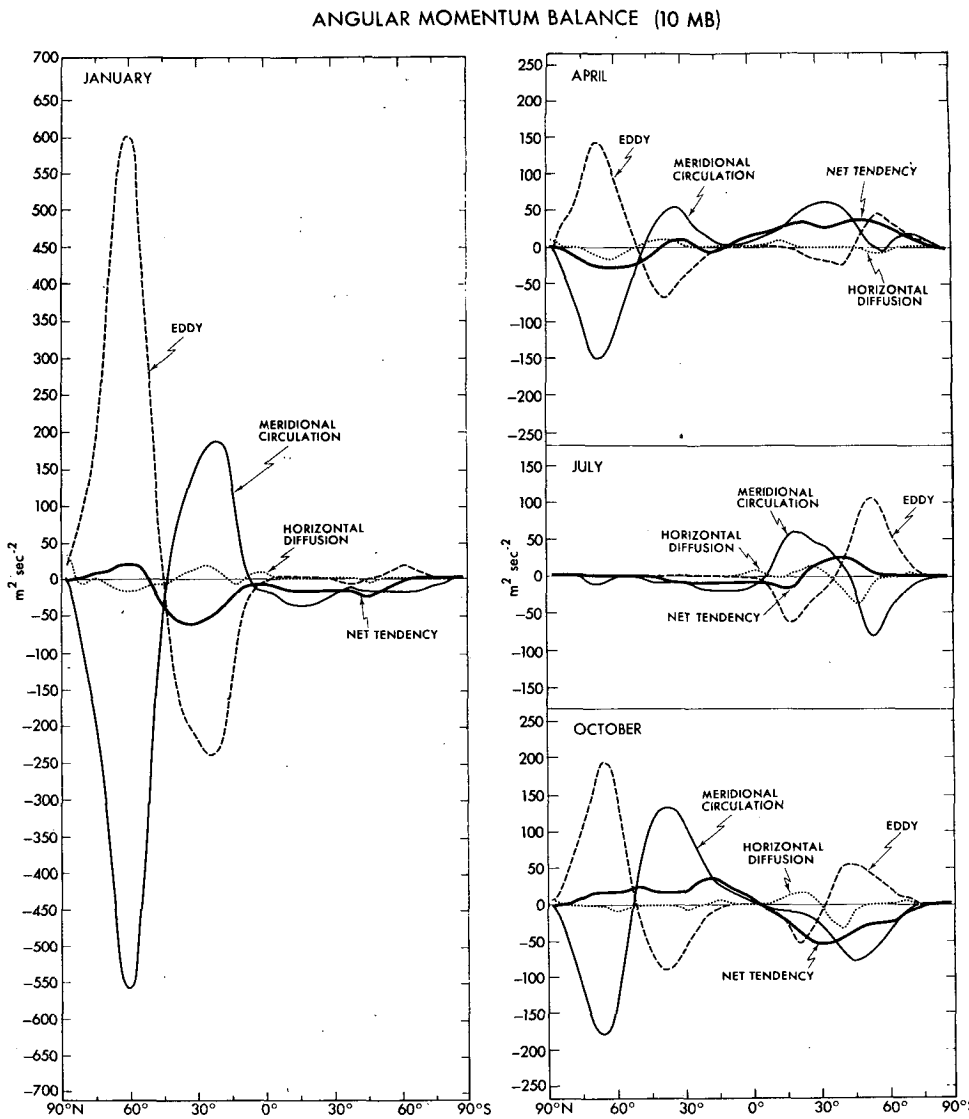

FIG. 7.1. The annual, zonal mean budget of angular momentum ($m^2 s^{-2}$) among various components, i.e., flux convergence by horizontal and vertical meridional circulation, flux convergence by horizontal and vertical large-scale eddies, horizontal diffusion and net tendency, at the 10 mb level of the model.

shows that a planetary wave in a vertical shear flow has no effect on the zonal motion unless at least one of the following conditions is satisfied:

1) The phase velocity of the given elementary planetary wave equals the speed of the mean zonal wind (i.e., critical levels are present).

2) Radiative or diffusive damping of the planetary waves takes place.

3) The amplitude or the phase velocity of the planetary waves change with time.

4) Nonlinear effects are significant.

Eliassen and Palm (1960) obtained a similar result for stationary gravity waves. Holton (1974) showed that this result is also applicable in the large-scale, nongeostrophic case where the Richardson number of the zonal flow is large. These results imply that the contribution of stationary waves (also time-independent, propagating waves) is compensated exactly by that of the induced meridional circulation unless any of the conditions listed are present. Therefore, it is reasonable that the compensation between the two components of momentum balance is particularly good in the Northern Hemisphere stratosphere during winter when the stationary eddies account for most of the eddy kinetic energy. However, the large compensation described above does not occur during periods when the shape and the intensity of the polar vortex rapidly changes with time. This often occurs in the model stratosphere due either to drastic changes in the tropospheric forcing or to some of the other situations listed above.

One of the interesting characteristics of Fig. 7.1 is the pronounced interhemispheric difference in the balance terms. The magnitude of the contributions of both meridional circulation and large-scale eddies during winter in the Northern Hemisphere is much larger than those in the Southern Hemisphere. As shown in Sections 5 and 6, both the meridional circulation and large-scale eddies in the Northern Hemisphere are much more pronounced than their Southern Hemisphere counterparts and account for the interhemispheric differences in the budget of angular momentum described above.

In the summer stratosphere of the model, strong compensations between mean cell and eddies do not take place. Furthermore, the magnitude of the contributions of both meridional circulation and large-scale eddies is very small. As described in Section 5, very weak equatorward flow appears at the 10 mb level during the first half of summer, and is responsible for strengthening the easterly currents which occupy the summer stratosphere. In short, the summer hemisphere budget of angular momentum at the 10 mb level essentially consists of the contribution of the meridional circulation producing a local change of angular momentum. It is interesting to note that the model of Cunnold *et al.* (1975) also successfully simulates the summertime easterlies, but with a meridional circulation quite different than the one obtained with this model.

The contribution of large-scale eddies is negligible in the summer. As will be shown in Section 9, much of the upward and meridional flux of energy by quasi-stationary planetary waves appears to be trapped near interfaces between mean easterlies and westerlies. This may explain why the disturbances in the regions of easterlies are very weak and contribute little to the budget of angular momentum in that area.

In Section 4, it is noted that the model successfully simulates the qualitative features of the seasonal variation of easterlies in the tropical stratosphere. According to the comparison between the seasonal variation of zonal wind (shown in Fig. 4.2) and meridional wind at 10 mb level of the model, the easterly jet in the equatorial stratosphere is at a maximum shortly after the cross-equatorial flow is strongest and most extensive (in January). This result is consistent with conservation of absolute angular momentum of the almost zonally symmetric flow in this region.

8. Heat balance

a. Annual mean

The annual average zonal mean heat balance of the lower stratosphere of the model is illustrated in Fig. 8.1, which shows the latitudinal distribution of various heat-balance components at the 110 mb level (note from Fig. 3.1 that the equatorial tropopause of the model is located around 110 mb). This figure indicates that the contributions of large-scale eddies and meridional circulation tend to compensate each other outside the tropics. A similar tendency of compensation was noted earlier in the results from the numerical model of Manabe and Hunt (1968), and was also discussed in an observational study by Mahlman (1969b). As discussed previously, large-scale quasi-stationary eddies can induce (under certain conditions) a meridional circulation which compensates for their own contribution to the change in the zonal mean temperature. According to Fig. 8.1, however, there is a significant imbalance between the two components. The net dynamical effect helps maintain the warm temperature in middle and high latitudes despite radiative cooling.

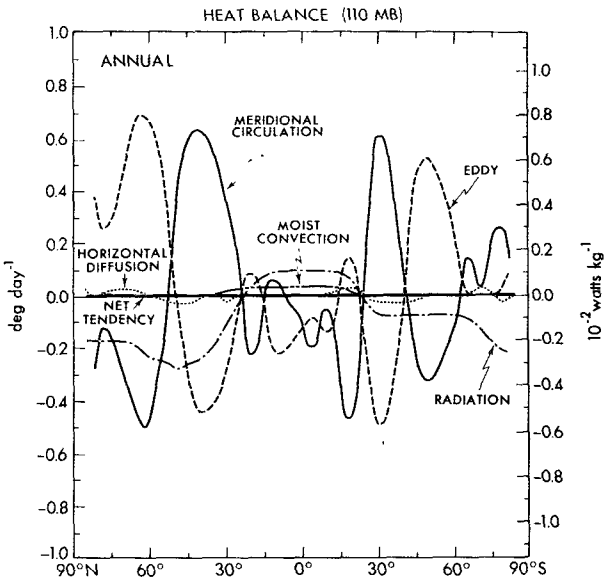

FIG. 8.1. Latitudinal distribution of the contributions of various heat balance components to the annual mean rate of temperature change at 110 mb in the model atmosphere, including meridional circulation, large-scale eddies, radiation, horizontal diffusion, moist convection and net tendency. Units in K day^{-1} and 10^{-2} W kg^{-1}.

In the model tropics, the compensating relationship such as that described above is not evident, though the distribution of the two contributions tend to be negatively correlated with each other. In this case both the meridional circulation and eddies contribute a cooling effect, and are responsible for the minimum temperature at the equatorial tropopause at the 110 mb level.

In the preceding sections, some of the mechanisms responsible for a lack of complete compensation between the contributions of eddies and the induced meridional circulation are discussed. However, there are other possible mechanisms for an imbalance. For example, meridional circulation in the stratosphere may be forced from the troposphere rather than induced by stratospheric disturbances (Kuo, 1956). It is probable that the upward zonal mean motion at the model equatorial tropopause is forced by heat of condensation releases in the model tropics.

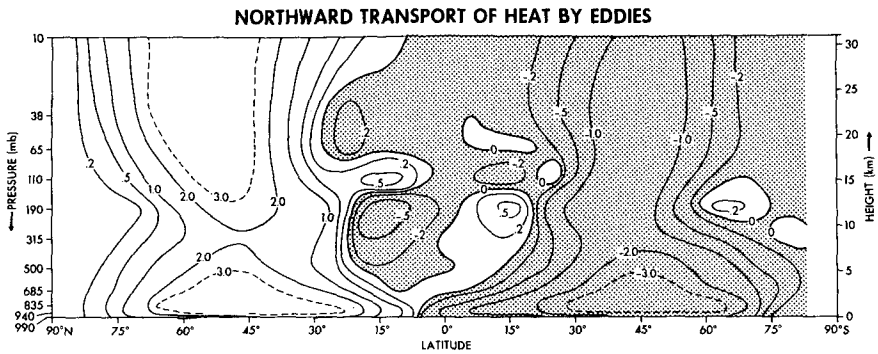

FIG. 8.2. Latitude-height distribution of the annual mean northward transport of heat by large-scale eddies in the model atmosphere. Units in 10^{11} J m^2 kg^{-1} s^{-1}.

Consistent with the discussion of meridional circulation in Section 5, Fig. 8.1 indicates that the heat balance at the 110 mb level in the polar region of the model stratosphere contains significant interhemispheric asymmetries. In the arctic region of the model, the net radiative cooling is overbalanced by an eddy flux convergence which induces an indirect meridional circulation and accompanying adiabatic cooling. On the other hand, the radiative cooling in the model antarctic region is balanced mainly by the heating due to meridional circulation.

The role of large-scale eddies in maintaining the latitudinal distribution of zonal mean temperature in the lower stratosphere was first emphasized by White (1954). Based upon an analysis of radiosonde data, he emphasized the importance of counter-gradient, poleward flux of heat in the heat budget of the lower stratosphere. Fig. 8.2 shows the latitude-height distribution of the northward eddy heat transport in the model atmosphere. This figure clearly indicates that, in the stratosphere, large-scale eddies transport heat poleward in both hemispheres, thus contributing to the general increase of temperature with increasing latitude. Note that the eddy flux of heat in the stratosphere of the Northern Hemisphere is significantly larger than that of the Southern Hemisphere.

Some interesting features of the distribution in Fig. 8.2 are the presence of local maxima of the poleward heat transport away from the equatorial tropopause at the 110 mb level in the model tropics. On the other hand, equatorward heat transport occurs in the upper troposphere. Analyzing the structure of disturbances in this model, Hayashi (1974) found that the so-called mixed Rossby-gravity-type wave and Rossby-type wave predominate in the model tropics. According to his analysis, the structures of these waves are such that they can account for the distribution of eddy heat transport described above. Consequently, these waves seems to be responsible for the cooling of the equatorial tropopause discussed earlier in this subsection.

The vertical distribution of various heat balance components at the model equator is shown by Fig. 8.3. This figure indicates that the sum of the contribution of solar heating and moist convective heating yields large heating in both troposphere and stratosphere, but very little heating around the level of the equatorial tropopause. There is little doubt that this feature is partly responsible for the temperature minimum at the equatorial tropopause of the model.

The dynamical effect also plays a significant role in maintaining the vertical distribution of temperature in the model tropics. According to Fig. 8.3, the large-scale eddies heat the upper troposphere and cool the equatorial tropopause, and thus act to intensify the temperature minimum at the equatorial tropopause. As previously noted, tropical eddies such as Rossby-type waves and mixed Rossby-gravity-type waves predominate in the model upper troposphere and the lower stratosphere and are responsible for these effects. Fig. 8.3 also indicates that at the equatorial tropopause of the model the meridional circulation produces a cooling effect.

The net effects of solar absorption, moist convection and large-scale atmospheric motion consist of intense heating of both stratosphere and troposphere and weak cooling of the layer around the equatorial tropopause. Since the annual mean atmosphere is in quasi-thermal equilibrium, these effects should be compensated by the remaining thermal process, i.e., terrestrial radiation. This implies that the contribution of the terrestrial radiation should consist of the cooling of both troposphere and stratosphere and weak heating of the layer around the tropopause. The temperature profile, which yields the vertical distribution of heating (or cooling) by terrestrial radiation described above, should contain a sharp minimum around the equatorial tropopause. Such a temperature minimum at the equatorial tropopause is evident in Fig. 3.1, which shows the latitude-height distribution of the zonal mean temperature in the model atmosphere.

The results described here are qualitatively similar to those obtained by Manabe and Hunt (1968), except that the cooling due to large-scale eddies is substantially less in their model than in the present model. In

their study they emphasized the importance of meridional circulation in maintaining the minimum temperature at the equatorial tropopause, but did not discuss the contribution of large-scale eddies. It is probable that the existence of the equatorial wall and the lack of selective heating by condensation in their model eliminated the mixed Rossby-gravity-type wave, and reduced the intensity of other tropical disturbances in their model atmosphere.

In this context it is interesting to note the results of a theoretical study by Dickinson (1971). Adopting the equatorial β-plane approximation, Dickinson obtained an analytic solution for the zonal mean circulation in response to sources of heat and momentum

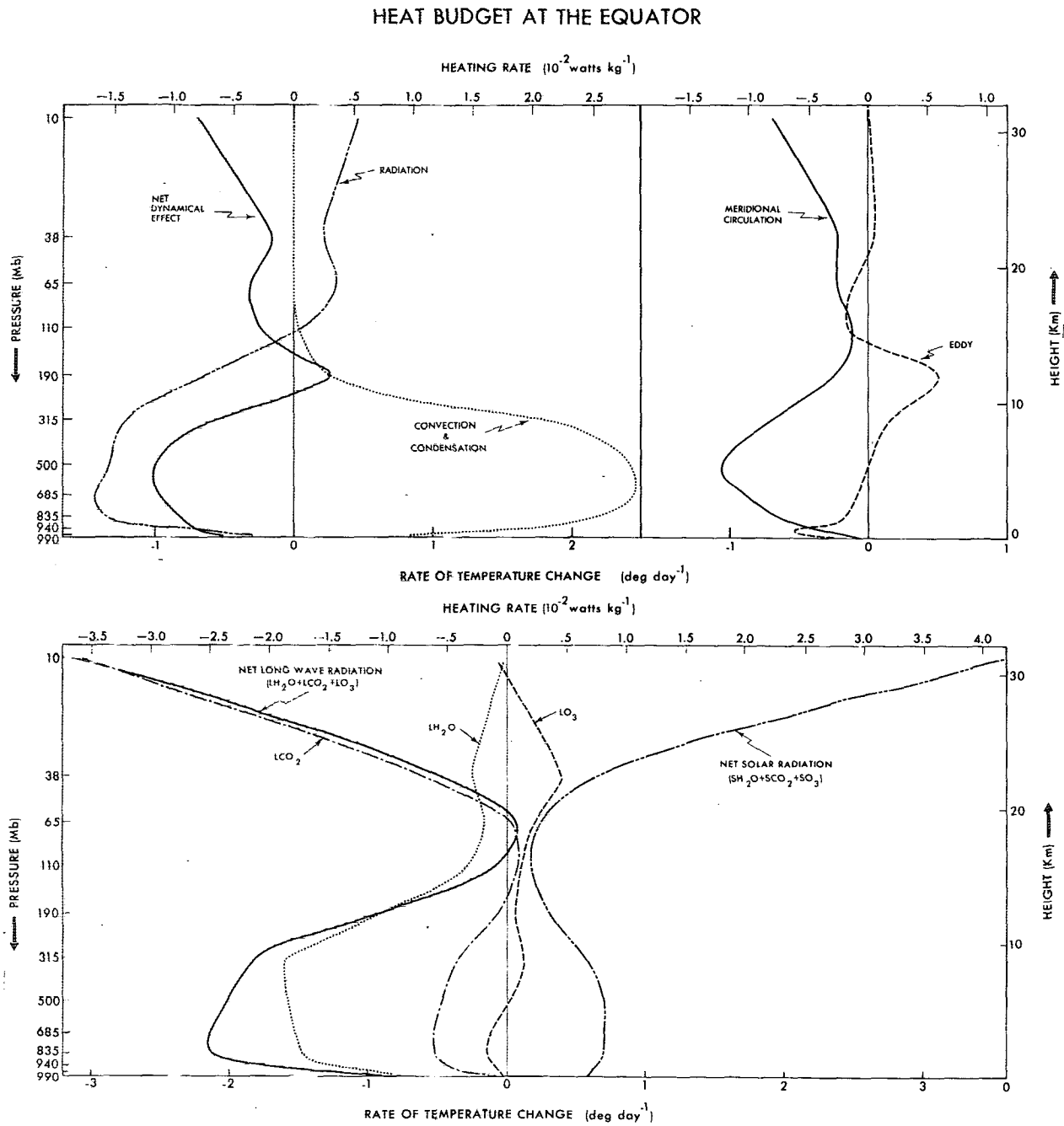

FIG. 8.3. Vertical distributions of the contributions of various heat balance components to the annual mean rate of temperature change at the model equator. Units in K day^{-1} and 10^{-2} W kg^{-1}. Top left: dynamics, radiation, convection and condensation; top right: meridional circulation, large-scale eddies; bottom: net longwave radiation, LH_2O, LCO_2, LO_3 and net solar radiation. Here L and S denote longwave radiation and solar radiation, respectively.

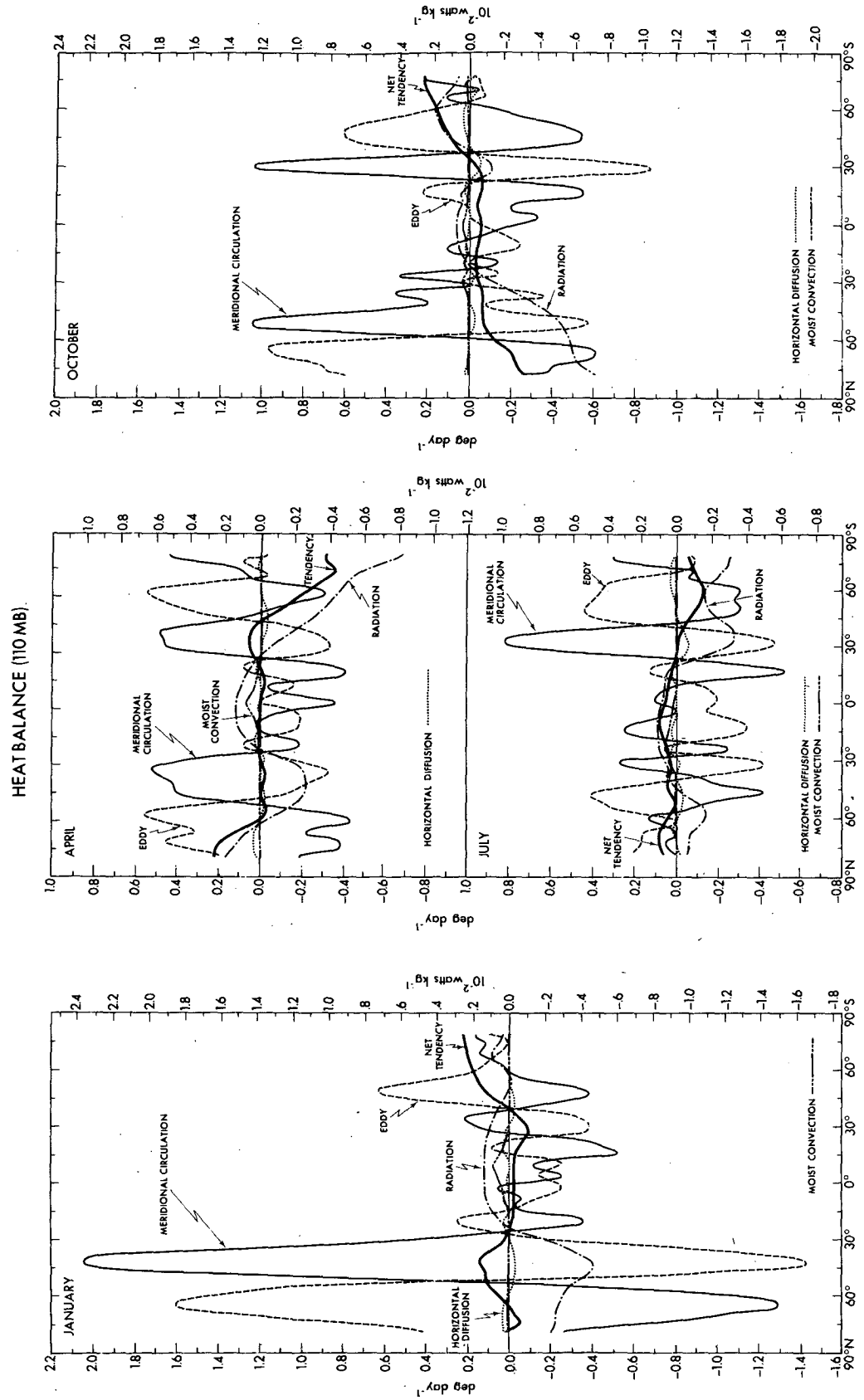

FIG. 8.4. Latitudinal distribution of the contribution of various heat balance components to the monthly mean rate of temperature change at the 110 mb level of the model. Units in K day^{-1} and 10^{-2} W kg^{-1}. For further detail, see caption for Fig. 8.1.

(the convergence of the transport of momentum by large-scale eddies being regarded as a momentum source). His solution predicts a minimum temperature at the equatorial tropopause which results from adiabatic cooling in the upward branch of the Hadley cell. His theory, however, does not take into consideration the effect of heat transport by large-scale eddies.

b. Seasonal variation

The seasonal variation of the heat budget in the lower stratosphere of the model may be inferred from Fig. 8.4, which shows the latitudinal distributions of various heat-balance components at the 110 mb level during four typical months of the year. By comparing this figure with Fig. 3.3, which shows the seasonal variation of zonal mean temperature at 110 mb, one can identify the important heat-balance components during each season of the year.

In high latitudes, the sign of the rapid changes of temperature during spring and fall is essentially determined by the net radiative heating and cooling. Since the effect of large-scale eddies tends to compensate that of meridional circulation, the net effect of large-scale motion is significantly less than the radiative effect. In general, large-scale motion tends to moderate heating (or cooling) due to radiative transfer in high latitudes of the model.

In middle latitudes, the zonal mean temperature in the lower stratosphere is warmest during winter when the intensity of solar radiation is at a minimum (see Fig. 3.3). Fig. 8.4 shows that in winter the rate of warming due to meridional circulation is significantly larger than the rate of cooling due to eddy flux divergence. This allows for the maintenance of the relatively warm temperature despite significant radiative cooling. In this context it is interesting to note that in both winter hemispheres the latitude of highest temperature at 110 mb is located at the position of strongest descent in the meridional circulation. In the Northern Hemisphere this position is about 45°N, while in the Southern Hemisphere, it is nearer 38°S. It is also worth noting that the seasonal variation of the contribution of meridional circulation is approximately in phase with the variation of the zonal mean temperature. Although the contribution of the meridional circulation is opposed by that of large-scale eddies, the former is significantly larger than the latter, and acts to maintain the seasonal variation of temperature despite the opposition by radiative effects.

In the tropical region of the model the temperature in the lower stratosphere is at a minimum around March, and is at a maximum around August as shown in Fig. 3.4. The general features of the equatorial temperature variation shown in this figure do not correspond with the seasonal variation of solar heating shown in the lower part of Fig. 8.5. This result suggests that the seasonal variation of temperature in the lower stratosphere of the model tropics is controlled by the effect of large-scale motion. Reed and Vleck (1969) pointed out that, in the lower stratosphere of the tropics, the temperatures in both hemispheres are observed to vary in phase. If the earth's surface were precisely the same in both hemispheres, they argue that the annual cycle would have to be of opposite phase in the two hemispheres and that there would be no annual temperature cycle at the equator. Therefore, they attribute the annual variation of temperature at the equator to interhemispheric differences in the characteristics of the earth's surface. Based upon results from the numerical experiment of Manabe and Hunt (1968), Reed and Vlcek further speculated that variation of meridional circulation is chiefly responsible for the temperature variation in the lower stratosphere. This is also consistent with the results obtained from the model of Dickinson (1971), mentioned earlier. Unfortunately, those studies did not consider the effect of heat transport by large-scale eddies.

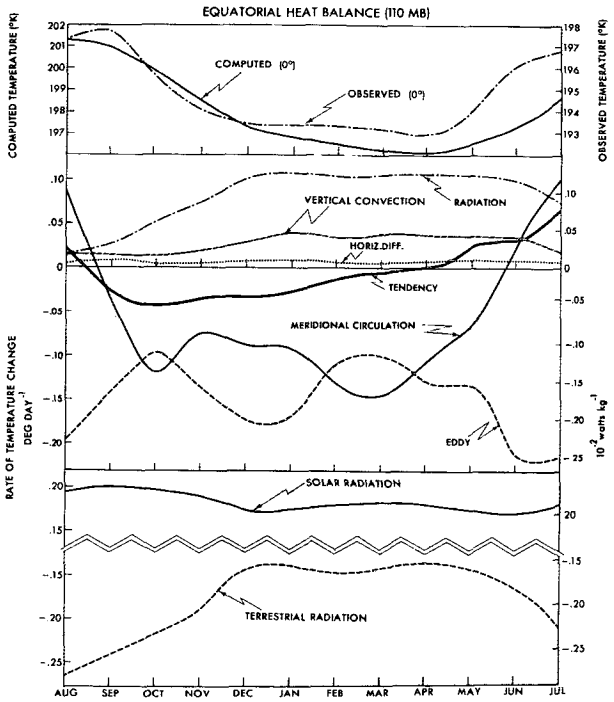

FIG. 8.5. Seasonal variation of the contributions of various heat balance components to the monthly mean heating rate at 110 mb in the model tropics. Units in K day^{-1} and 10^{-2} W kg^{-1}. The values are averaged over the latitude belt 15°S to 15°N. (Data source: Oort and Rasmussen, 1971.)

The seasonal variation of the heat balance at the model equatorial tropopause is given in Fig. 8.5. These results should be regarded with caution, because as discussed in the beginning of Section 7, the analysis fails to satisfy the condition of heat balance. Nevertheless, this figure indicates that the meridional circulation produces strong cooling in March when the temperature is lowest, and produces a warming effect in

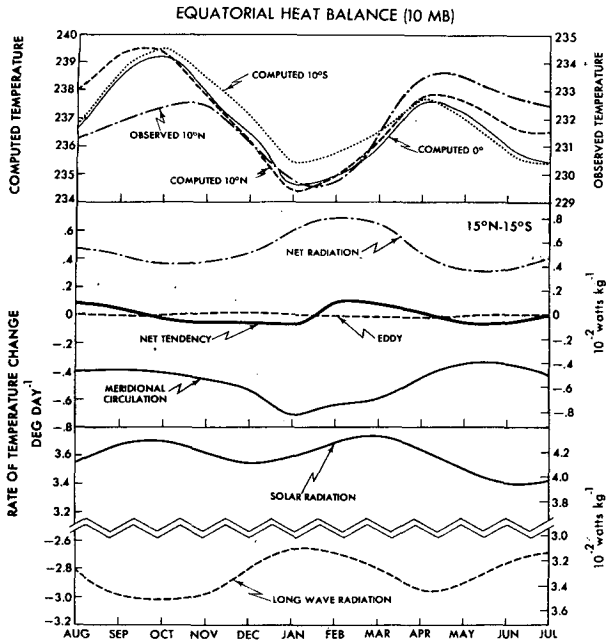

FIG. 8.6. As in Fig. 8.5 except at 10 mb in the model tropics. (Data source: Labitzke *et al.*, 1972.)

June–August when the temperature is highest. On the other hand, the contribution of the eddies is to produce the least cooling in March and the greatest cooling in June–August, thus acting in opposition to the effect of the meridional circulation. The net dynamical effect appears to be controlling the seasonal change in temperature, despite the radiative damping.

In the mid-stratosphere of the model the general features of temperature variation at the equator are significantly different from those in the lower stratosphere. Fig. 8.6 shows that at 10 mb, the temperature is a maximum in October and April, and at a minimum in January and July. This quasi-semiannual variation is in reasonable agreement with the features of the actual atmosphere. This figure also indicates that the seasonal variation of temperature is determined by small differences between the opposing contribution of meridional circulation and that of net radiation. At this level, where eddy kinetic energy is very small, the contribution of large-scale eddies is also very small. By comparing the seasonal variation of zonal mean temperature described above with those of the various heat balance components, one can see that the temperature is lowest in January, when the cooling effect of the meridional circulation is maximum, and that it is next lowest in July when the heating due to the absorption of solar radiation is relatively weak. These results suggest that the contributions of both the meridional circulation and solar radiation have comparable effects upon the simulated seasonal variation of temperature in the equatorial mid-stratosphere. On the other hand, terrestrial radiation acts to reduce the seasonal temperature variation. Recently, Fritz (1974) analyzed the seasonal variation of the emission from the mid-stratosphere, as measured by the so-called Satellite Infrared Spectrometer. He concluded that solar heating alone cannot account for the observed changes of radiance unless the thermodynamic effect of large-scale motion is taken into account. His results appear to be consistent with the results of this study.

9. Eddy kinetic energy balance

The equation for zonal-mean eddy kinetic energy on an isobaric surface is

$$\frac{\overline{\partial k_E}^{\lambda}}{\partial t} = [-\overline{D(k_E)}^{\lambda} + \overline{\langle k_Z \cdot k_E \rangle}^{\lambda} - \overline{\mathbf{V}' \cdot \nabla \phi'}^{\lambda} + \overline{\mathbf{V}' \cdot \mathbf{F}'}^{\lambda}], \quad (9.1)$$

where

$$k_E = k_T - k_Z, \quad (9.2)$$

$$k_T = \tfrac{1}{2}(u^2 + v^2), \quad (9.3)$$

$$k_Z = \tfrac{1}{2}[(\bar{u}^{\lambda})^2 + (\bar{v}^{\lambda})^2], \quad (9.4)$$

$$\overline{D(\,)}^{\lambda} = \frac{1}{a\cos\theta}\frac{\partial}{\partial\theta}(\cos\theta\,\overline{v(\,)}^{\lambda}) + \frac{1}{\partial p}\overline{(\omega(\,)}^{\lambda}) \quad (9.5)$$

$$\langle k_Z \cdot k_E \rangle = \left(\frac{\bar{u}^{\lambda}}{\cos\theta}\right)\overline{D(u'\cos\theta)}^{\lambda} + \bar{v}^{\lambda}\left(\overline{D(v')}^{\lambda} + \frac{\tan\theta}{a}\overline{(u'^2)}^{\lambda}\right). \quad (9.6)$$

In these equations t represents time, a the radius of the earth, $\mathbf{V}$ the horizontal wind vector, u and v the eastward and northward components of the wind, p the pressure, ω the vertical p-velocity, θ the latitude, ϕ the geopotential height and $\mathbf{F}$ is the frictional force vector. The λ and prime superscripts indicate a zonal mean and its deviation, respectively. In the following discussion, the sum of the first two terms in the brackets of (9.1) will be called the nonlinear term, the third term the production term (of eddy kinetic energy) and the fourth term the eddy kinetic energy dissipation term. The nonlinear term consists of two terms: $(-\overline{D(k_E)}^{\lambda})$, which represents the flux convergence of eddy kinetic energy, and $(\overline{\langle k_Z \cdot k_E \rangle}^{\lambda})$, which represents energy transfer from zonal to eddy kinetic energy. The production term may also be divided into two parts:

$$-\overline{\mathbf{V}' \cdot \nabla \phi'}^{\lambda} = -\overline{\omega'\alpha'}^{\lambda} - \overline{D(\phi')}^{\lambda}, \quad (9.7)$$

where α is specific volume. The first part represents the conversion of eddy available potential energy to eddy kinetic energy, and the second part represents

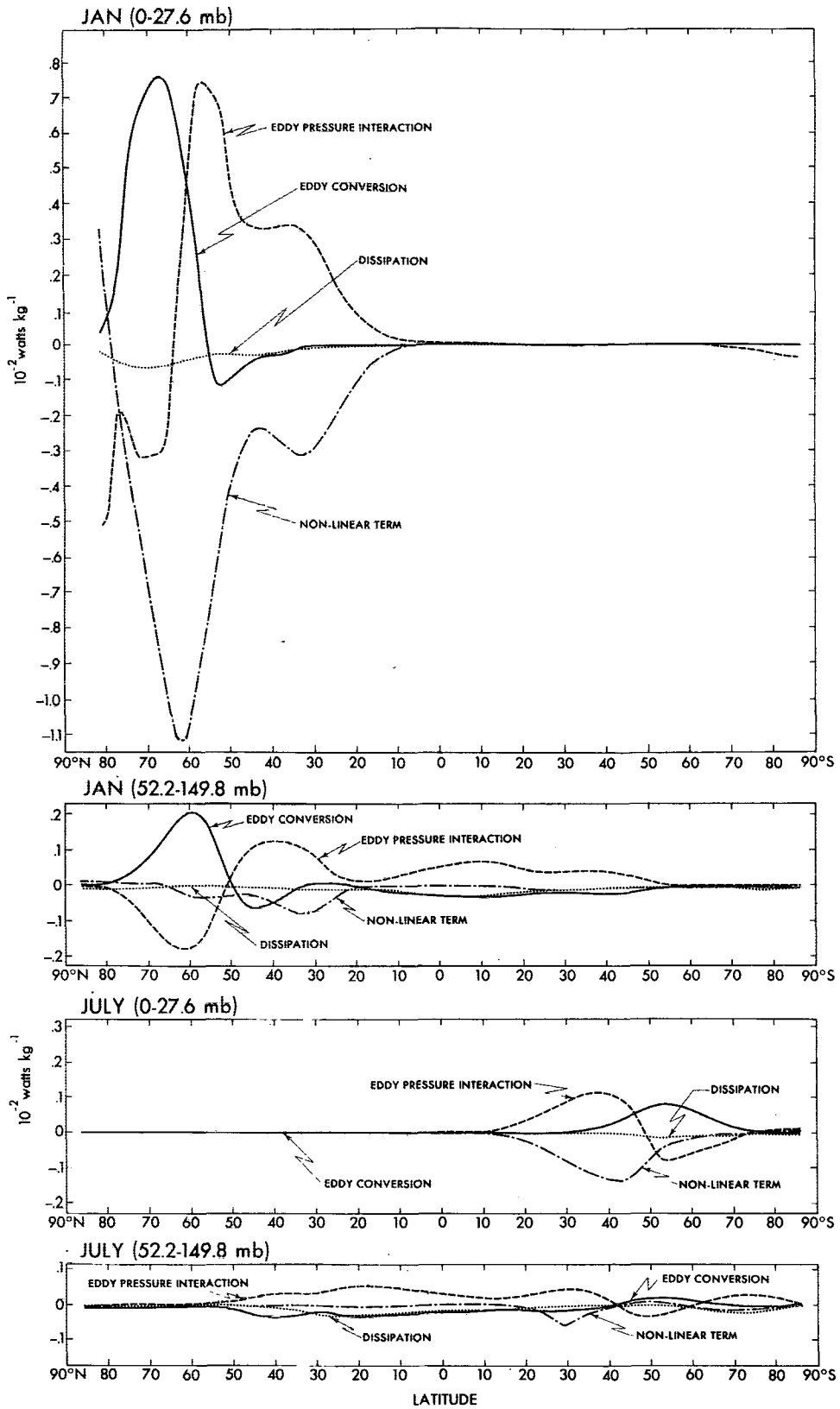

FIG. 9.1. Latitudinal distributions of various components of the budget of eddy kinetic energy in the model atmosphere, i.e., eddy pressure interaction, eddy conversion, nonlinear term, dissipation. From the top to the bottom: 0–27.6 mb layer in January, 52.2–149.8 mb layer in January, 0–27.6 mb layer in July, 52.2–149.8 mb layer in July. Units in 10^{-2} W kg^{-1}.

convergence of energy due to eddy flux of geopotential (eddy pressure interaction).

Fig. 9.1 shows latitudinal distributions of various components of the eddy kinetic energy budget during January and July for a middle stratospheric volume (0–27.6 mb) and a lower stratospheric volume (52.2–149.8 mb). This figure shows a very large difference in the magnitude of the eddy kinetic energy balance components between winter and summer. Also, consistent with Fig. 6.1, the Northern Hemisphere winter eddy activity is much larger than in Southern Hemisphere winter. In order to identify the mechanisms responsible for these differences, the energetics for the two seasons in the two hemispheres will be discussed in some detail.

In winter the eddy conversion in the top layer of the model stratosphere (i.e., 0–27.6 mb) is positive in high latitudes and is mostly negative elsewhere. On the other hand, the contribution of eddy pressure interaction to the production of eddy kinetic energy is negative in very high latitudes and is positive in the remaining latitudes. The net effect is that both eddy conversion and eddy pressure interaction supplement each other in producing eddy kinetic energy during winter. The eddy kinetic energy thus produced is in turn transferred to zonal kinetic energy through barotropic processes. Averaged over the hemispheric domain, the direction of energy transfer in the top layer of the model stratosphere during winter is as follows:

$$A_E \rightarrow k_E \rightarrow k_Z \rightarrow A_Z$$
$$\uparrow$$
Troposphere

where A_Z and A_E represent zonal and eddy available potential energy, respectively. This result is in qualitative agreement with observational results on the energetics of the middle stratosphere in January (e.g., Dopplick, 1971; Newell *et al.*, 1974).

In the model lower stratosphere Fig. 9.1 shows that the magnitudes of the energy budget components are much less than those in the top layer. In addition, the relative contribution of the nonlinear term decreases markedly. The results given in Fig. 9.1 are very different from those presented by Kasahara and Sasamori (1974). Their results give (for the 18–36 km layer) a positive eddy conversion from 0° to 50°N and a negative eddy conversion from 50° to 90°N, almost completely opposite to the results shown in Fig. 9.1.

The positive contribution of pressure interaction in the model stratosphere during winter is provided mainly by upward flux of energy from the model troposphere. This is evident in Fig. 9.2 which shows, as an example, the latitude-height distributions of vertical and meridional flux of energy through eddy flux of geopotential in January. According to this figure, the upward eddy flux of geopotential predominates in high latitudes of the Northern Hemisphere. It is a major source of energy in the top layer of the model stratosphere where the horizontal eddy flux of geopotential transports energy toward lower latitudes. In the lower part of the model stratosphere (i.e., 52.2–149.8 mb layer) the upward flux of energy from the troposphere converges in middle and low latitudes, and contributes to the production of eddy kinetic energy.

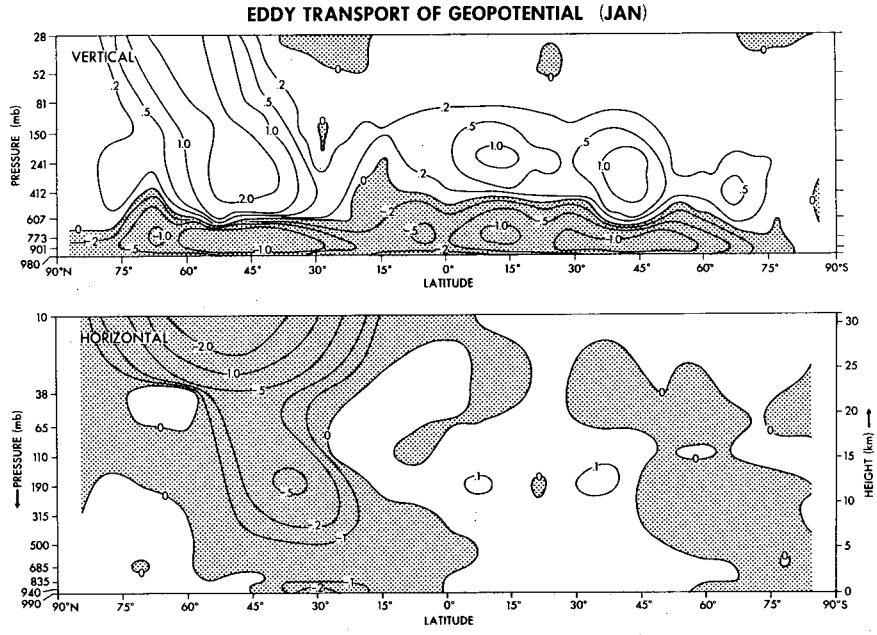

FIG. 9.2. Latitude-height distributions of the eddy transport of geopotential in the model atmosphere during January. Top: vertical flux (W m^{-2}); bottom: northward flux (10^{11} J m^2 kg^{-1} s^{-1}).

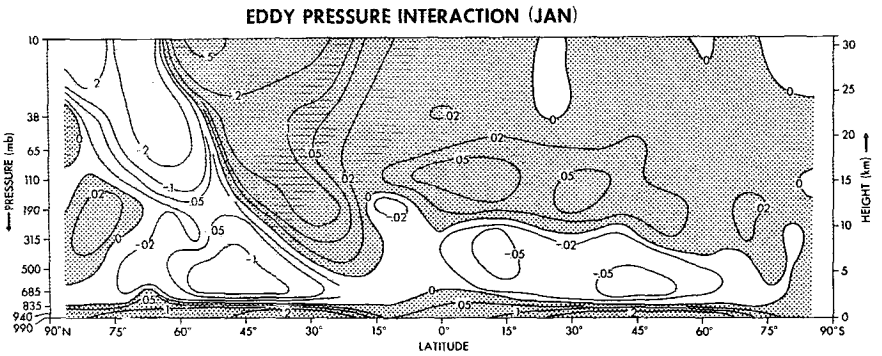

FIG. 9.3. Latitude-height distribution of the rate of change of eddy kinetic energy due to eddy pressure interaction in the model atmosphere during January. Units in 10^{-2} W kg^{-1}.

In the summer hemisphere the magnitudes of both horizontal and vertical fluxes are negligible in the part of the stratosphere where easterly winds prevail. This is apparently because energy flux tends to be prevented from reaching the easterly regions due to a phenomenon similar to that known as "critical-layer absorption." As pointed out by Eliassen and Palm (1960), Charney and Drazin (1961) and Charney (1969), the energy flux due to stationary (or slowly traveling) waves should become small in the neighborhood of the interface between mean westerlies and mean easterlies. Fig. 9.2 reveals that at the 10 mb level the southward flux of energy markedly decreases around 25°N where the zonal wind reverses direction. In the Southern Hemisphere, the upward flux almost vanishes near the boundary of the easterly region. Fig. 9.1 implies that a similar phenomenon appears in the stratosphere of the Northern Hemisphere during July. In short, eddy kinetic energy in the easterly region of the summer stratosphere is strongly suppressed, probably due mainly to critical-layer-type absorption of the energy flow from the surrounding regions.

Matsuno (1970) discussed the structure of quasi-stationary disturbances which predominate in the Northern Hemisphere during the winter. The theoretical distribution of energy flux obtained from his study qualitatively resembles the distribution shown in Fig. 9.2, except that his flux penetrates into much higher layers of the atmosphere. Furthermore, the convergence of upward eddy transport of energy and the magnitudes of other energy budget components at the 10 mb level of the present model appear to be significantly exaggerated relative to the observed data of Newell *et al.* (1974). These comparisons suggest that the present study suffers from a large distortion of the energy fluxes near the top model level due to the coarse vertical resolution there, as well as to the use of the "lid" boundary condition.

Fig. 9.3 shows the latitude-height distribution of the convergence of energy flux due to eddy pressure interaction during January. Convergence occurs in middle and low latitudes where energy flows toward decreasing zonal currents in agreement with the Eliassen-Palm relationship (see Figs. 4.1, 9.2 and 9.3). In view of the fact that stationary waves predominate in the Northern Hemisphere part of the model stratosphere during winter (see Section 6), it is reasonable that the Eliassen-Palm relationship obtained for stationary waves approximately holds there.

The latitude-height distribution of January-mean eddy conversion in the model atmosphere is shown in Fig. 9.4. According to this figure, eddy conversion is negative in the lower stratosphere of the Southern (summer) Hemisphere, where the eddy kinetic energy

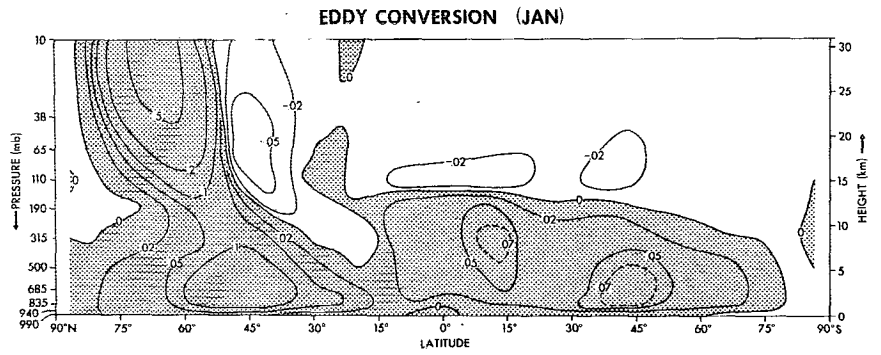

FIG. 9.4. Latitude-height distribution of eddy conversion in the model atmosphere during January. Units in 10^{-2} W kg^{-1}.

TABLE 1. Global mean eddy kinetic energy budget of the model stratosphere averaged over a 1-year period. Units in 10^{-4} W kg^{-1}.

Pressure interval (mb)	Nonlinear term	Eddy conversion	Eddy pressure interaction	Eddy dissipation	Computational imbalance
0.0– 27.6	−4.50	1.13	3.19	−0.66	0.84
27.6– 52.2	−0.86	0.66	0.90	−0.76	0.06
52.2– 80.8	−0.65	−0.11	1.40	−0.98	0.34
80.8–149.8	−0.95	−1.05	3.20	−1.30	0.10

is maintained by forcing from below (see Figs. 9.2 and 9.3). Eddy conversion is also negative in middle and low latitudes of the Northern Hemisphere, where energy flux comes from below and from higher latitudes. Eddy conversion is positive in high latitudes of the model Northern Hemisphere where the eddy-pressure-interaction flux is divergent. These eddy conversion results agree with those obtained in observational studies by Miyakoda (1963) and Dopplick (1971). It should be noted here that the region of positive conversion in the model stratosphere coincides approximately with the region of upward flux. Using the linear, adiabatic, quasi-geostrophic approximation it can be shown, where stationary disturbances transport energy upward and the westerly wind increases with height, that a positive conversion will occur (see, e.g., Hartmann, 1975). This relationship suggests that the positive conversion in high latitudes is not the manifestation of baroclinically unstable waves, but may be a result of quasi-stationary disturbances which tilt westward with height and transport energy upward (McIntyre, 1972).

An analysis of the seasonal variation of eddy kinetic energy budget in the top layer of the model (i.e., 0–27.6 mb layer) reveals that the contributions of both pressure interaction and eddy conversion vary in phase with the magnitude of eddy kinetic energy. For example, the eddy-pressure-interaction effect is at a maximum in the winter when eddy kinetic energy is largest. As noted earlier, positive eddy conversion in winter appears to be a manifestation of quasi-stationary disturbances which transport energy upward. In short, these results show the dominating influence of energy flux from the troposphere in controlling the seasonal variation of the eddy kinetic energy at the 10 mb level of the model stratosphere. Again, it should be noted that the contribution of this and other terms of energy budget appear to be significantly exaggerated because of the possible influences of the lid boundary condition and the coarse vertical resolution in the model middle stratosphere.

In the lower stratosphere of the model (i.e., 52.2–149.8 mb layer), the situation is significantly different. Although the contribution of eddy pressure interaction is positive throughout the year, it slightly increases during summer, probably because of the critical-layer-type absorption mentioned earlier. On the other hand, the contribution of eddy conversion has a seasonal variation which is in phase with the variation of eddy kinetic energy in the model lower stratosphere. The eddy conversion is positive (maximum) in winter and negative during the remainder of the year.

Table 1 contains the global mean values of various components of the budget averaged over a one-year period. According to this table, the magnitudes of these components are much larger in the upper model stratosphere (i.e., 0–27.6 mb layer) than in the lower model stratosphere (i.e., 52.2–149.8 mb layer). This is probably due to the distortion at the top level as mentioned previously. The annual mean budget in the upper stratosphere is essentially maintained between the positive contributions of eddy pressure interaction and eddy conversion and the negative contributions of the transfer from eddy to zonal kinetic energy and dissipation. However, in the lower stratosphere this budget is maintained between the positive contributions of eddy pressure interaction and the negative contributions of eddy conversion and dissipation. The annual mean energy budget in the model lower stratosphere is in qualitative agreement with the results obtained by Oort (1964) for the actual lower stratosphere.

One of the interesting features of the energy budget in the model stratosphere is its large interhemispheric differences. Fig. 9.1 shows that the magnitudes of eddy conversion, eddy pressure interaction and the nonlinear term during Northern Hemisphere winter are much larger than those in the Southern Hemisphere's winter. In addition, the contributions of these terms predominate in the Northern Hemisphere at significantly higher latitudes than they do in the Southern Hemisphere. These results appear to be consistent with the interhemispheric differences in the distribution of eddy kinetic energy and angular momentum balance in the model stratosphere as described in the preceding sections.

It is shown in Section 6 that the partitioning of eddy kinetic energy into stationary and transient components is quite different between the two model hemispheres. Similar interhemispheric differences are evident in the corresponding partitioning of the energy budget components. Fig. 9.5 shows the latitude-height distributions of both stationary and transient components of the upward eddy flux of geopotential during January and July. In January the stationary component accounts for most of the upward flux of energy into the stratosphere in middle and high latitudes of the Northern Hemisphere. However, in July the transient component is responsible for major parts of the upward transport in middle latitudes of the Southern Hemisphere. As shown in Fig. 9.6, similar differences in partioning hold for the conversion of eddy potential energy into eddy kinetic energy. For example, the stationary component accounts for almost all eddy

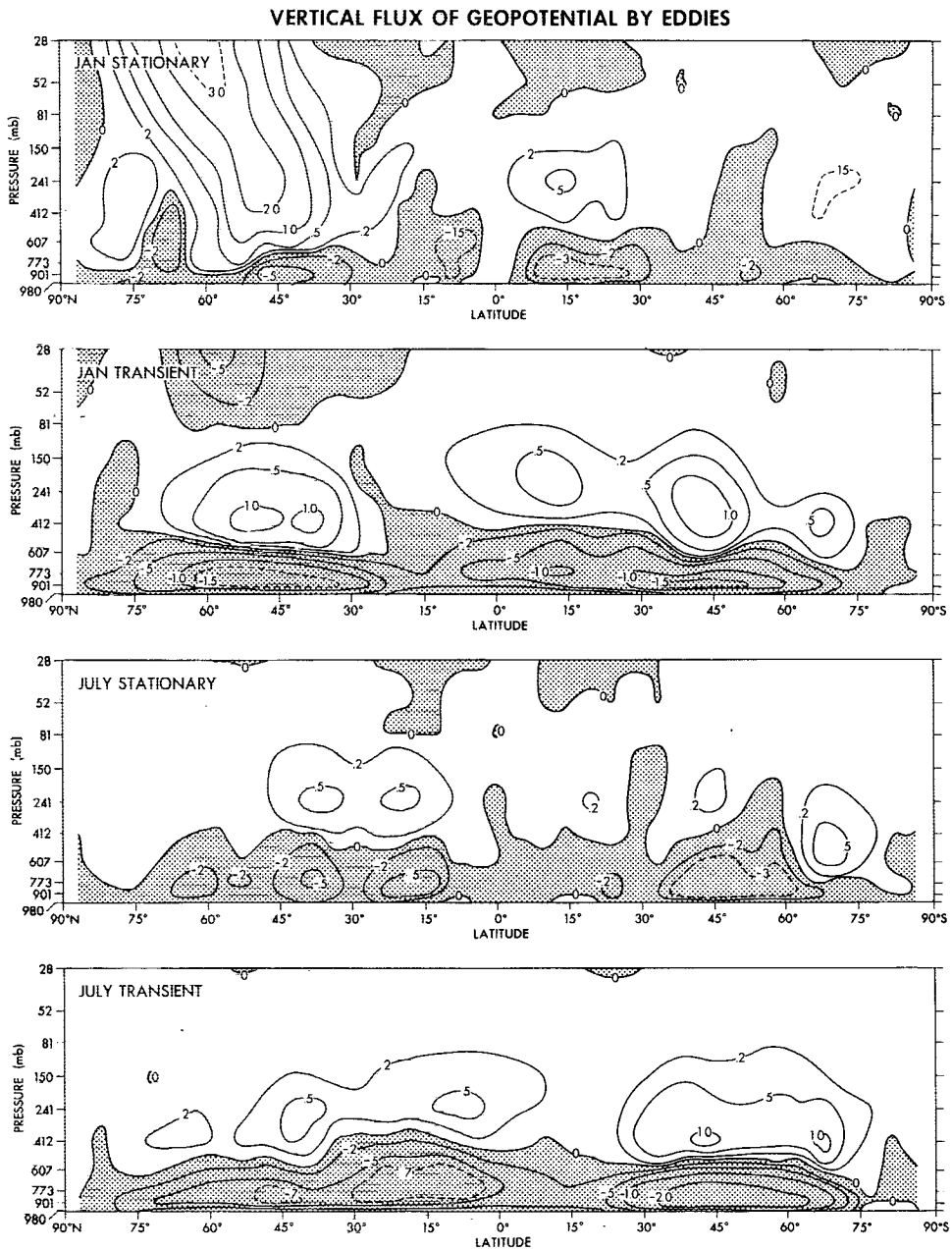

FIG. 9.5. Latitude-height distributions of upward flux of energy due to stationary and transient eddy flux of geopotential in the model atmosphere. From top to bottom: stationary eddy flux in January; transient eddy flux in January; stationary eddy flux in July; transient eddy flux in July. Units in W m^{-2}.

conversion in high latitudes of the Northern Hemisphere during January. In contrast the transient component is somewhat larger than the stationary component in the Southern Hemisphere during July. Obviously, the interhemispheric differences in the energy budget described above are responsible for the interhemispheric differences in the distribution of eddy kinetic energy in the model stratosphere as discussed in Section 6. Again, the distribution of large-scale mountain ranges appears to be the basic cause for these differences.

10. Structure of the stationary field

In Figs. 10.1, 10.2 and 10.3, the time-mean distributions of geopotential height and temperature for various isobaric surfaces in the model stratosphere are compared with those in the actual atmosphere. The observed maps for the Northern Hemisphere have been compiled by Crutcher and Meserve (1970) and those for the Southern Hemisphere were constructed by Taljaad *et al.* (1969) based upon results from the SIRS satellite as well as conventional data. To obtain sta-

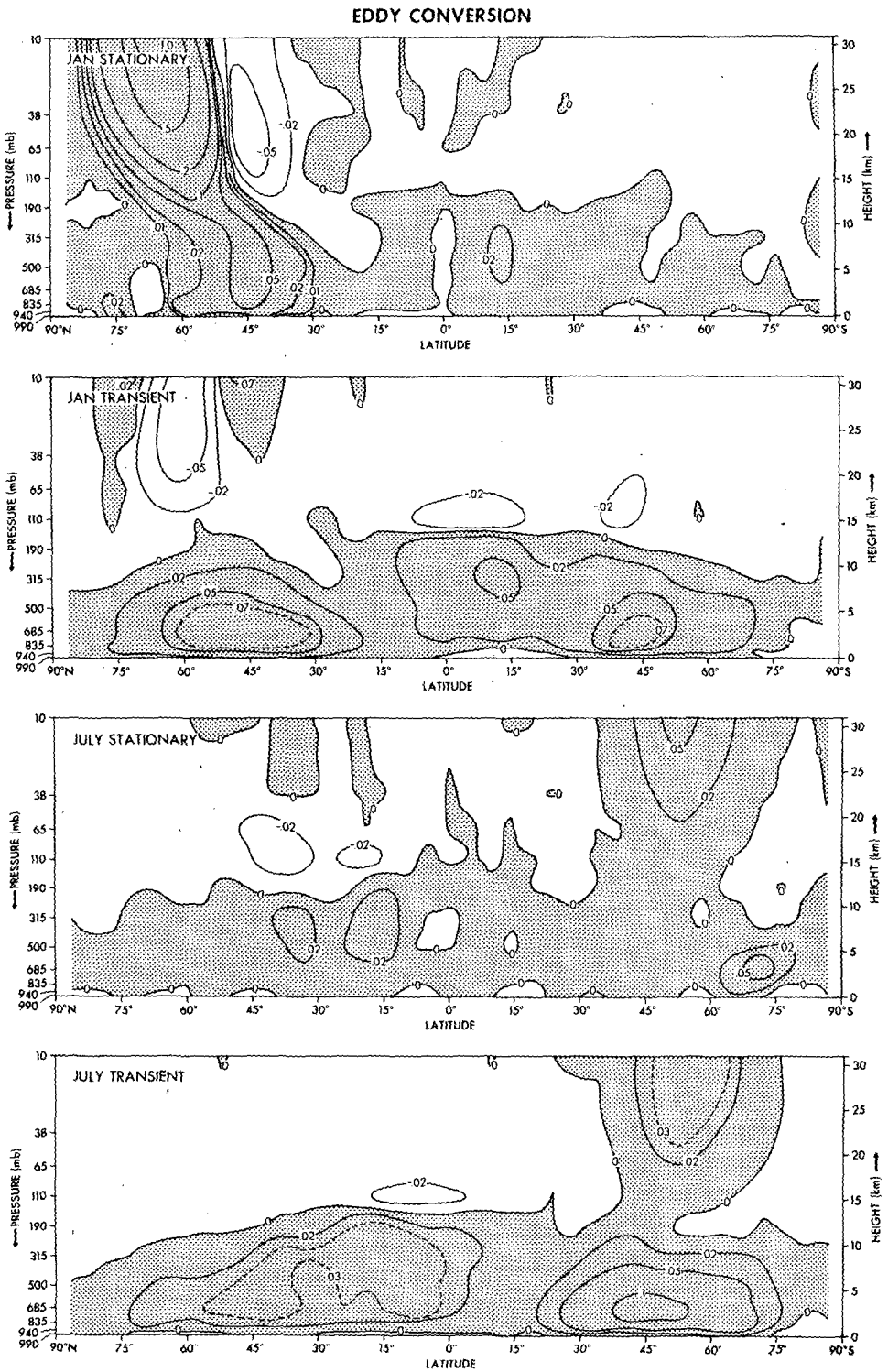

FIG. 9.6. Latitude-height distributions of the stationary and the transient component of eddy conversion in the model atmosphere. From top to bottom: stationary eddy conversion in January; transient eddy conversion in January; stationary eddy conversion in July; transient eddy conversion in July. Units in 10^{-2} W kg^{-1}.

tionary distributions independent of short-term fluctuations, both temperature and geopotential height are averaged over 3-month periods. The periods for which these maps are made are December–February and June–August.

In the model Northern Hemisphere at 10 mb, Fig.

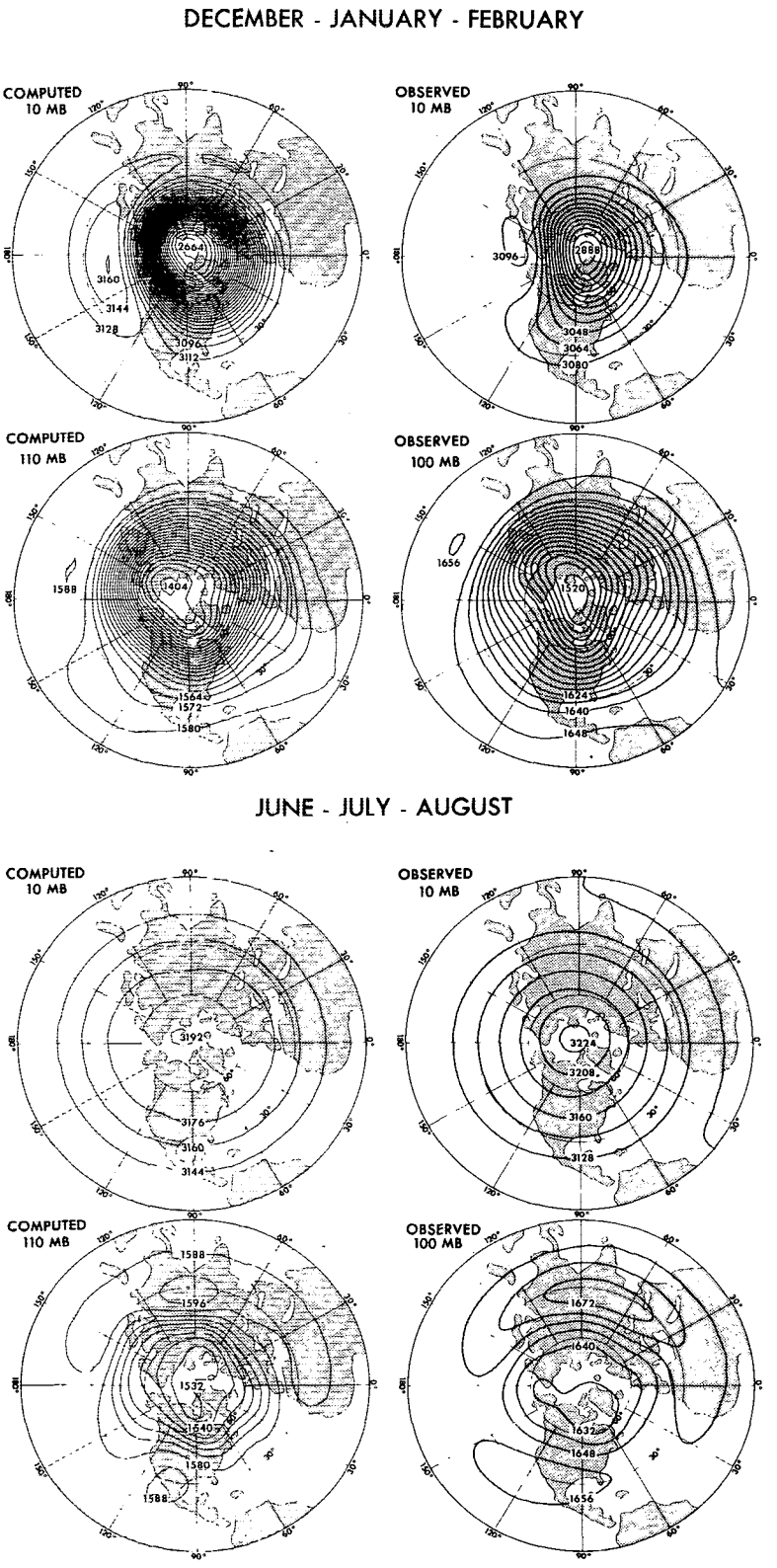

FIG. 10.1. Stereographic maps of quarterly mean geopotential height at 10 and 110 mb in the Northern Hemisphere. Upper half: December–February; lower half: June–August. Left: computed; right: observed. Units in dam. (Standard geopotential height difference between 110 and 100 mb is 390 m.)

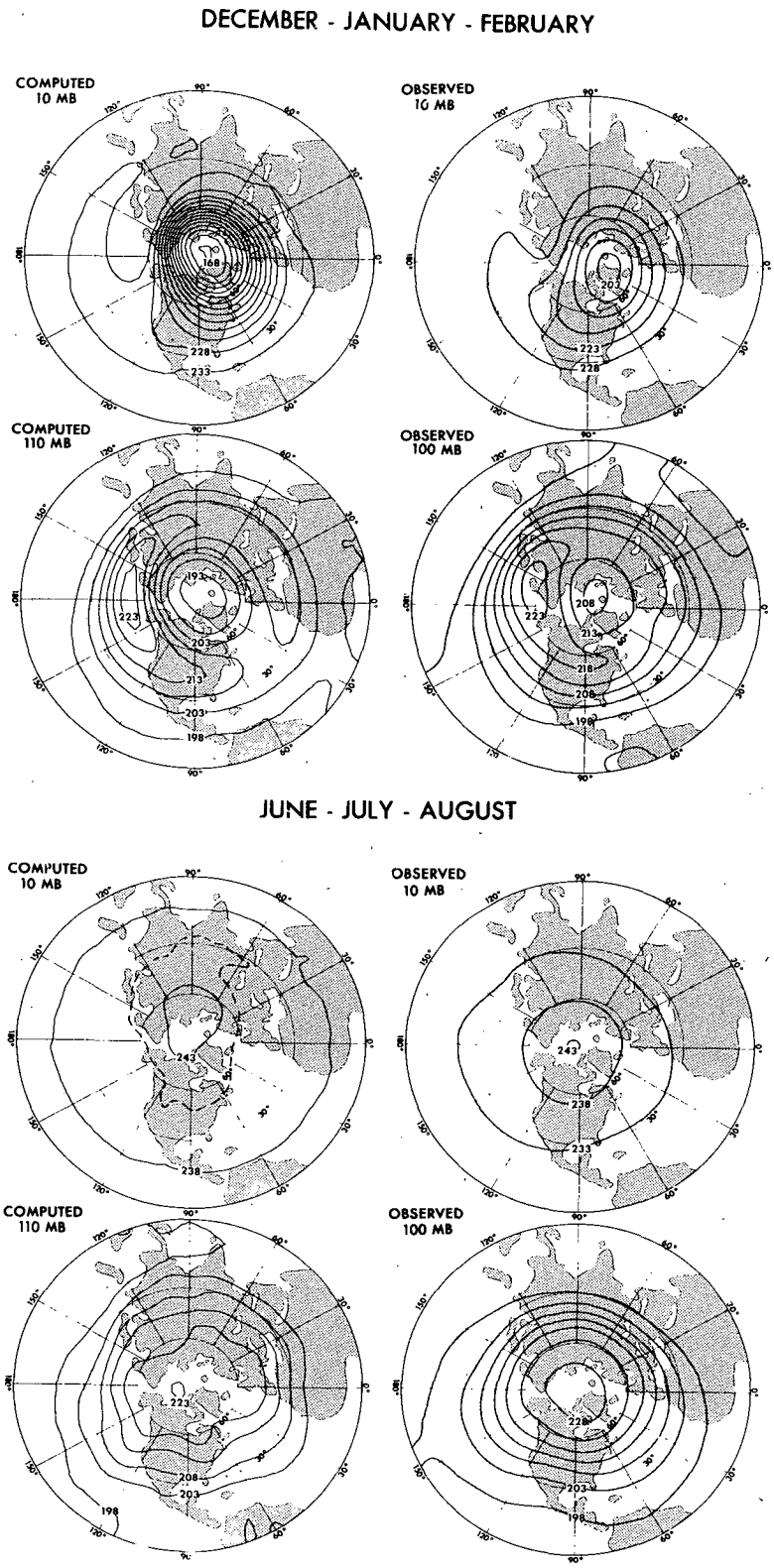

FIG. 10.2. As in Fig. 10.1 except for mean temperature (K).

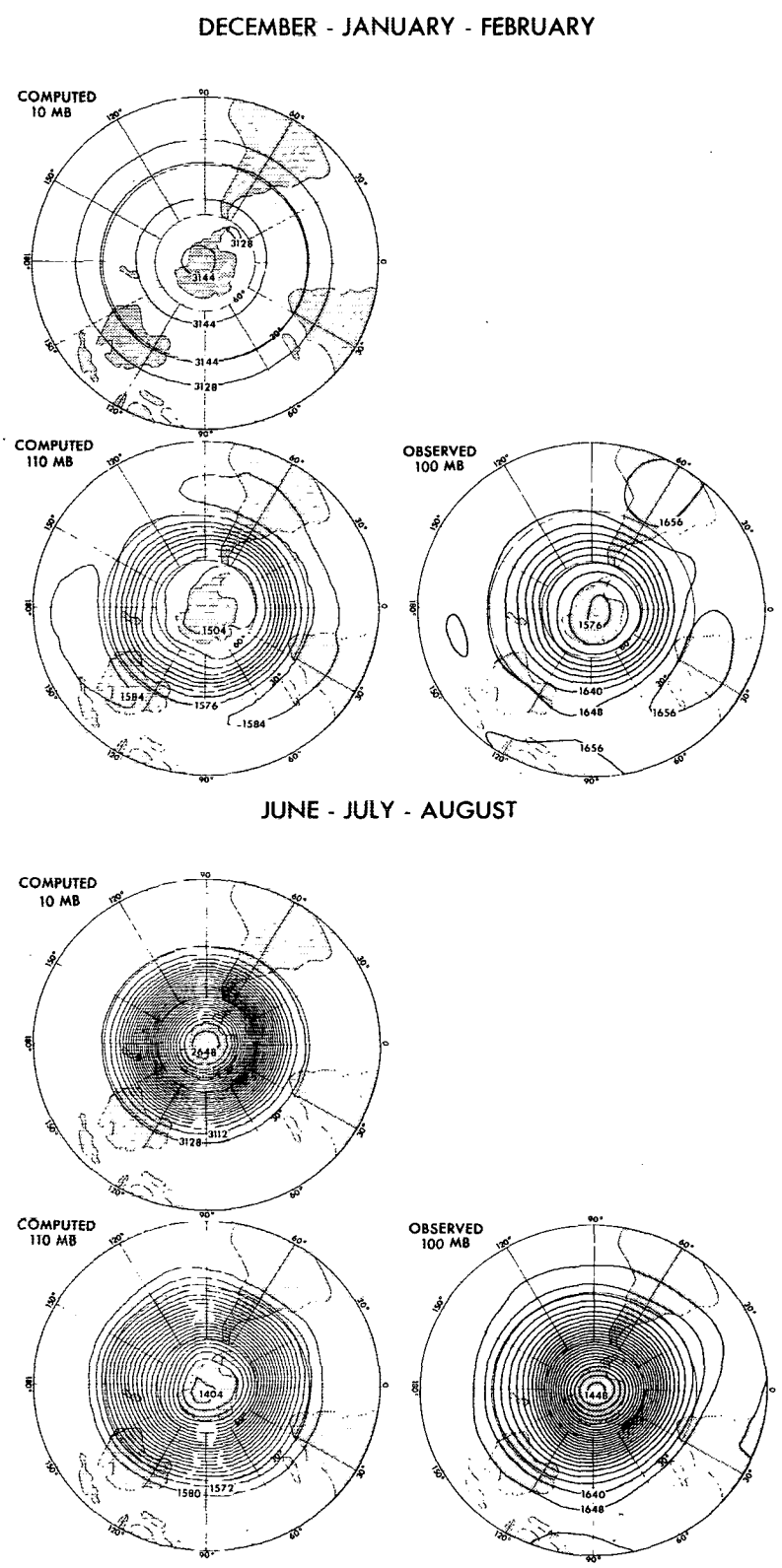

FIG. 10.3. As in Fig. 10.1 except in the Southern Hemisphere.

10.1 shows that a cold polar vortex prevails during winter. It is very intense and has an elongated shape with a distinct trough over the North American Continent. It is accompanied by an anticyclone over the North Pacific Ocean. In late spring the polar vortex weakens, moves out of the polar regions and is replaced by an anticyclonic vortex which occupies the entire Northern Hemisphere in summer. The summer vortex is much weaker than the winter vortex and has an almost concentric shape. These features of the seasonal evolution of quasi-stationary vortices in the model stratosphere are in qualitative agreement with those in the actual stratosphere. However, there are quantitative differences. For example, the intensity of the winter cyclone is much too strong and the summer anticyclone is somewhat weaker than observed. The excessive development of the winter cyclone mentioned above is consistent with the excessive intensity of zonal mean wind in the model winter stratosphere, as described in Section 4.

Comparison of Figs. 10.1 and 10.3 indicates that the cyclonic vortex which prevails during the winter in the Southern Hemisphere is more axial symmetric relative to the pole than the winter vortex in the Northern Hemisphere. This is consistent with the pronounced interhemispheric differences discussed in previous sections.

Distributions of geopotential height at the 110 mb level are also included in Fig. 10.1. In winter the cyclonic vortex at 110 mb is more extensive and more concentric than the vortex at 10 mb. It has major troughs over Europe, the eastern part of the North American continent and along the east coast of Asia. As the season changes from winter to summer, this cyclonic vortex weakens and shrinks significantly. At the same time anticyclonic vortices appear in the subtropics. They are centered over the southern parts of the Eurasian Continent and the North American Continent. These general features of the seasonal variation of the model lower stratospheric circulation are in qualitative agreement with those of the actual atmosphere. However, the intensity of the cyclonic vortex is exaggerated in both winter and summer and the anticyclonic vortex in the model subtropics appears to be too weak in comparison with the actual atmosphere.

In the Northern Hemisphere winter, Fig. 10.2 reveals that the area of warm temperature over the North Pacific, and the area of cold temperature over the Arctic at 110 mb correspond roughly to the Aleutian anticyclone and the polar cyclone, respectively, at 10 mb. In the Northern Hemisphere summer the isotherms at 110 mb are more axial symmetric relative to the North Pole than during winter. The increase of temperature with increasing latitude at 110 mb is consistent with the anticyclonic, easterly flow at 10 mb.

The results presented in this section and in previous sections all point to significant interhemispheric differences in the simulated winter stratospheric circulation. Similar differences are evident in the observed distributions. A significant portion of these major interhemispheric circulation differences appears to be mainly attributable to the occurrence of the stationary Aleutian anticyclone and its concomitant displacement of the cyclonic vortex away from the pole.

Considerable insight can be gained into the nature of these mid-stratospheric phenomena by examining some of the time-averaged features of the lower stratosphere. In Fig. 10.4 the model January and July mean 190 mb isotachs and 110 mb isotherms are shown. For January the 190 mb isotachs reveal the presence of a strong jet stream maximum near Japan. Note that this maximum is much larger than the winds at other longitudes. In July a strong 190 mb jet is present in the Southern Hemisphere. In this case the longitudinal variation of wind speed is far smaller.

Fig. 10.4 also shows that these 190 mb jet stream systems are associated with marked effects on the temperature in the model lower stratosphere. In the Northern Hemisphere during January a pronounced warm region is present at 110 mb in the central Pacific. In the Southern Hemisphere during July the warm region is weaker and much more zonally symmetric. It is interesting to note, however, that the zonal-mean mid-latitude warm regions at 110 mb (shown in Fig. 3.2) are very similar in each winter season. Also, Fig. 3.3. shows that these warm belts are warmer in mid-winter than during any other season. A more detailed analysis shows that these local warm regions are sustained dynamically by descending vertical motion poleward of the jet stream core. Near the east coast of Asia in January this sinking is particularly intense, and is associated with strong negative vorticity advection as the air passes to the north of the jet maximum. The warmest temperature in the central Pacific is located near the point of zero vertical velocity (greatest downward excursion along the trajectory). Part of this temperature excess is then advected poleward on the east side of the long-wave trough, and part is destroyed locally by radiative processes.

It is interesting to note the contrast between this "explanation" of the mid-latitude warm region and that implied by the zonal mean heat balances shown in Fig. 8.4. The zonal mean balances "explain" the warm region as resulting from a slight dominance of meridional circulation heating over cooling by radiation and eddy flux divergence. On the other hand, Fig. 10.4 implies strongly that the local sinking motion producing the warm region leads to a sinking in the zonal mean simply because most of the local compensating rising motion tends to occur further poleward. This effect is quite clear in Northern Hemisphere January where the calculated compensation in Fig. 8.4 between mean cell and eddies is nearly three times as large as that obtained for Southern Hemisphere July.

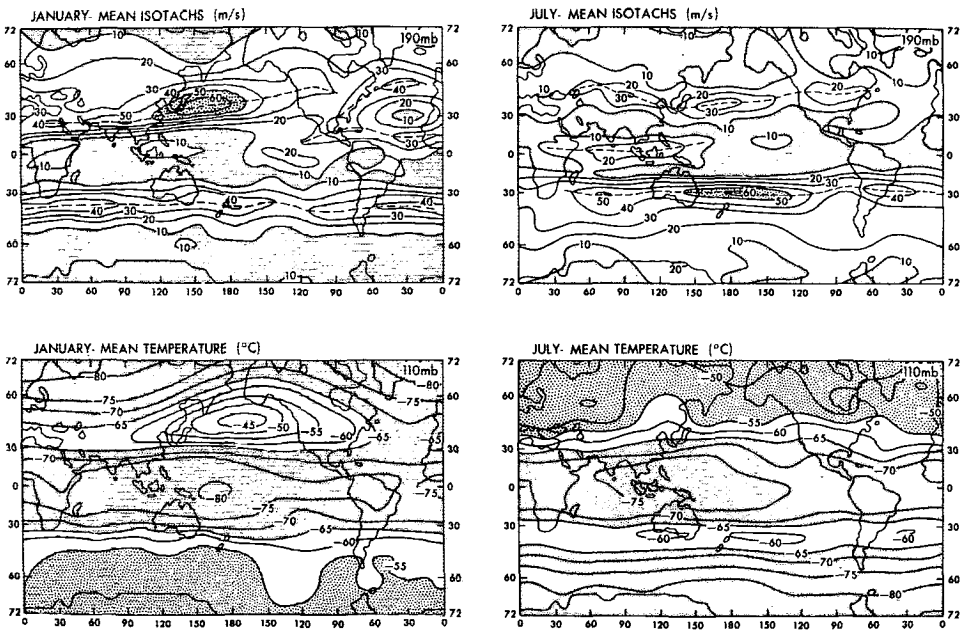

FIG. 10.4. Mecator maps of simulated January mean (left) and July mean (right) isotachs (top) and temperature (bottom). Isotach units: m s^{-1}; temperature units: °C.

A different perspective on the lower stratosphere structure can be obtained by viewing Fig. 10.5, which shows a latitude-height cross section of the January mean wind speed and temperature along 150°E, a longitude near the Japan jet. This cross section shows many features which agree very closely with those of the actual atmosphere. For example, the location of the Japan jet core, its magnitude and wind shears all agree closely with observations. Moreover, the mean temperature structure south of 60°N and below 38 mb appears to be well simulated. The points of disagreement involve the region above 200 mb near 70°N which is systematically too cold by about 10 K and the upper boundary south of the stratospheric jet stream where the temperature is too warm by about 5 K. These two deficiencies operate together to produce an unrealistically intense stratospheric jet stream.

The descending motion responsible for producing the warm region above and poleward of the tropospheric jet so evident in Figs. 10.4 and 10.5 is found to be related to a transverse circulation about the jet which yields rising motion on the equatorward side of the jet and sinking motion on the poleward side. This transverse circulation is also reflected in the model-computed fields of potential temperature, potential vorticity and tracer mixing ratio. Further, it is consistent with the diagnostic studies of Krishnamurti (1961) for the subtropical jet stream and Mahlman (1973b) for the polar-front jet stream. Such a transverse circulation is thermally direct in the troposphere and thermally indirect in the lower stratosphere. Since this Northern Hemisphere jet stream is relatively local and is thus largely an "eddy" effect, such a transverse circulation and the temperature field of Fig. 10.5 are consistent with the stationary eddy conversion field shown in Fig. 9.6. Also, the upward flux of geopotential implied by this circulation is consistent with the vertical flux of geopotential by stationary eddies portrayed in Fig. 9.5.

The horizontal scale of this jet stream is such that a zonal harmonic analysis will reveal the most power to be in planetary wavenumbers 0, 1 and 2. The upward propagation of energy associated with this system is thus compatible with the theoretical prediction of

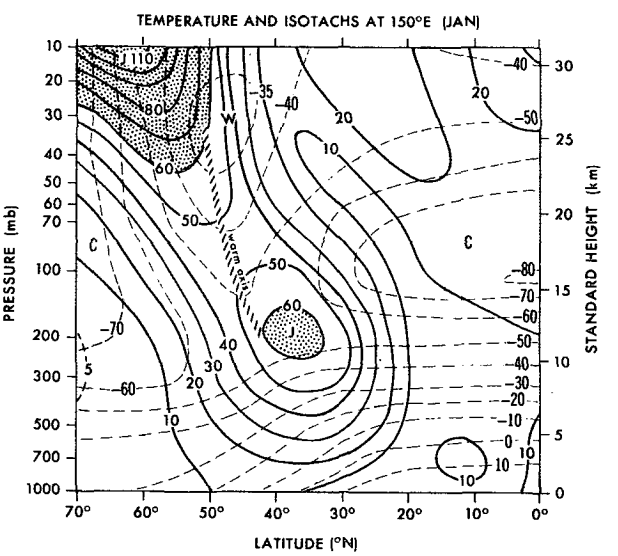

FIG. 10.5. Local cross section of simulated January mean temperature (°C, dashed lines) and isotachs (m s^{-1}, solid lines) at 150°E.

Charney and Drazin (1961) that only the very largest scale eddies can produce efficient upward energy flux in the winter stratosphere.

At 110 mb the induced warm region is associated with a trough off the east coast of Asia (see Fig. 10.1). However, this relatively deep layer of warm temperatures leads systematically to a hydrostatic build-up of high pressure, thus producing the Aleutian anticyclone. In east–west cross section this effect appears as a westward tilt of the 110 mb ridge located near the west coast of North America. This is consistent with the observational results of van Loon *et al.* (1972). In north–south cross section it appears as a poleward tilt of the 110 mb mid-Pacific anticyclone.

These discussions thus reveal that many diagnostic results from this simulation are directly and indirectly associated with a single phenomenon, the tropospheric jet stream near Japan. Based upon the results from their numerical experiments. Manabe and Terpstra (1974) concluded that major mountain ranges in the Northern Hemisphere, particularly the Himalayas, are responsible for this local maximum in the intensity of the jet stream. It is therefore probable that the interhemispheric asymmetries in topography cause the interhemispheric differences in the zonality of the jet stream in the troposphere, and accordingly, those features of the stratospheric circulation described in this section.

11. Summary and conclusions

a. Reversal of zonal wind and angular momentum budget

It has been shown that the global atmospheric circulation model described in this paper is capable of simulating the stratospheric seasonal reversals of zonal wind between westerlies in winter and easterlies in summer. It is also shown that, with the exception of the summer season and the equatorial region, the angular momentum budget in the model stratosphere is maintained between opposing contributions from the meridional circulation and large-scale eddies. A small difference between the two contributions essentially accounts for the seasonal change in zonal currents. It appears to be significant, however, that the seasonal variation of the intensity of the polar vortex is in phase with the variation of angular momentum convergence due to large-scale eddies, but out of phase with the contribution of the meridional circulation and diffusion. These results suggest that eddies exert a dynamical control on the seasonal variation of the intensity of the polar vortex. Further studies are required for the determination of the exact nature of this control.

During the summer large-scale eddies in the model are almost nonexistent. Consequently, the eddy contribution to the angular momentum budget is negligible. Very weak equatorward flow of the meridional circulation extends all the way to the subtropics of the winter hemisphere during the first half of the summer season and contributes to intensification of the zonal easterly vortex in the summer mid-stratosphere of the model.

b. Eddy kinetic energy budget

The seasonal variation of eddy kinetic energy in the model stratosphere has been examined by analysis of the kinetic energy budget. This analysis reveals that, with the exception of the summer season, the hemispheric mean budget of eddy kinetic energy in the top layer of the model (i.e., 0–27.6 mb layer) is maintained between the positive contributions of pressure interaction and eddy potential energy conversion, and the negative contribution of energy transfer from eddy to zonal kinetic energy and dissipation. It is suggested that this positive conversion is not a manifestation of baroclinic instability, but is indicative of the structure of planetary waves with upward energy propagation. The contributions of both eddy pressure interaction and eddy conversion are at a maximum during winter, when the level of eddy kinetic energy is highest in the model stratosphere. These results indicate the dominating influence of the stratosphere-troposphere interaction (through eddy pressure interaction) upon the seasonal variation of eddy kinetic energy in the mid-stratosphere.

There is strong evidence that the convergence of the upward energy flux (eddy pressure interaction) and other components of the eddy kinetic energy budget in winter at the top computational level are exaggerated because of the influence of coarse resolution and the lid boundary condition. Therefore, the quantitative details of the energy budget described here should be regarded with reservation.

During the summer season the eddy kinetic energy in the region of mid-stratospheric easterlies is simulated to be extremely small. This is probably because the flux of energy from the surrounding westerly regions tends to experience critical-layer-type absorption in the vicinity of the $\bar{u}^{\lambda}=0$ line.

In the lower stratosphere (i.e., 52.2–149.8 mb layer) of the model the three energy balance components identified above again play a major role. However, the contribution of the nonlinear term is less important than in the upper layer. It should be noted that eddy conversion is positive during the winter only, and is negative during the remainder of the year. In short, the seasonal variation of eddy conversion is in phase with that of eddy kinetic energy in the lower model stratosphere.

c. Interhemispheric asymmetries

Major emphasis of this study has been placed upon analysis of the interhemispheric asymmetries in the model stratosphere. Some of these asymmetries are listed below.

1) In the Northern Hemisphere of the model, the winter polar vortex has an elongated shape with its center significantly away from the North Pole. This indicates that the vortex is predominantly composed of zonal wavenumbers 0, 1 and 2. In the Southern Hemisphere the polar vortex is more zonally symmetric than its Northern Hemisphere counterpart. Because of the predominance of quasi-stationary disturbances during winter, the amount of eddy kinetic energy in the Northern Hemisphere stratosphere is much larger than that in the Southern Hemisphere.

2) Most of the simulated interhemispheric differences in the winter stratosphere can be related to the very different structures of the tropospheric stationary jet streams in the two hemispheres. In the Southern Hemisphere the tropospheric jet is nearly zonally symmetric, while in the Northern Hemisphere an especially strong jet stream is observed off the east coast of Asia. In particular, the occurrence of the stratospheric Aleutian anticyclone in the Northern Hemisphere is shown to be a result of this structure.

3) The budgets of eddy kinetic energy in the model stratosphere during winter are quite different in the two hemispheres. For example, the eddy geopotential energy flux from the troposphere to the stratosphere due to quasi-stationary disturbances is much larger in the Northern Hemisphere than in the Southern Hemisphere. This accounts for the interhemispheric difference in the magnitude of eddy kinetic energy mentioned above. Other components of the energy budget such as eddy conversion and the transfer from eddy to zonal kinetic energy also exhibit large interhemispheric differences. Consistent with results from other numerical experiments, the interhemispheric difference in the magnitude of eddy pressure interaction appears to be related to the presence of major mountain ranges in the Northern Hemisphere of the model.

4) The winter meridional circulation in the model stratosphere also reveals large interhemispheric differences. In the Northern Hemisphere, a two-cell meridional circulation prevails during winter, whereas in the Southern Hemisphere a very weak third meridional circulation cell appears in the polar region. Furthermore, the meridional circulation intensity is considerably stronger in the Northern Hemisphere.

5) During winter, the stratospheric budget of angular momentum in the Northern Hemisphere of the model is maintained between the two almost compensating contributions of the meridional circulation and large-scale eddies. On the other hand, during Southern Hemisphere winter, the magnitudes of these two contributions are much reduced, and the compensating relationship is less evident. It is argued that this compensating relationship in the Northern Hemisphere stems from the predominance of quasi-stationary disturbances in which the contribution of eddies nearly compensates with that of the induced meridional circulation.

d. Thermal structure and heat balance

It has been shown that the global model successfully simulates many features of the stratospheric thermal structure and its seasonal variation. For example, the model reproduces the sharp minimum temperature at the equatorial tropopause, the so-called "tropopause gap" in the subtropics, and the general latitudinal increase in temperature in the lower stratosphere. In middle latitudes of the model the temperature of the lower stratosphere is at a maximum in winter and at a minimum in summer. It thus is completely out of phase with the contribution of heating due to the absorption of solar radiation. The seasonal variation of temperature at the equatorial tropopause of the model also does not follow the variation of solar radiation at the equator. It is at a minimum near March and at a maximum around August. These features of the seasonal variation of thermal structure in the model stratosphere are in good qualitative agreement with the observed variations.

An analysis of the heat budget indicates that, at the equatorial tropopause of the model, weak mean upward motion appears during most of the year and causes adiabatic cooling. In addition, tropical disturbances transport heat away from the equator against the zonal mean temperature gradient. Both these effects contribute to the cooling of the equatorial tropopause, where both solar heating and moist convective heating are very small. It is important to note that the seasonal variation of the temperature at the equatorial tropopause described above is almost in phase with the seasonal variation of the contribution of meridional circulation, but is out of phase with the contributions from the large-scale eddies. The net dynamical effect appears to be controlling the seasonal temperature change in opposition to radiative effects.

In the middle latitudes of the model lower stratosphere the adiabatic heating in the downward branch of the meridional circulation is at a maximum during winter. Although the seasonal variation of the contribution of the meridional circulation is out of phase with that of large-scale eddies, the former is significantly larger than the latter. Also, the net dynamical effect again dominates the radiative effect in determining the seasonal temperature variation.

e. Critical remarks

Although the model reproduces some of the basic features of the seasonal variation of the stratosphere as described above, significant progress is required before a fully satisfactory simulation of the stratosphere can be claimed. In fact, the model stratosphere represents one of the less realistic aspects of the simulation by the global model. One of the most serious difficulties

is that the westerlies in the model stratosphere are twice as strong as observed. Furthermore, the model fails to reproduce such interesting phenomena as the mid-winter sudden warming and the quasi-biennial reversal of zonal wind in the equatorial stratosphere. Unfortunately, the fundamental causes for these difficulties have not been conclusively identified. However, it is highly probable that the behavior of the highest computational level at 10 mb level is significantly distorted because of the coarse vertical resolution and the lid boundary condition imposed at the top of the model atmosphere. As emphasized in the earlier part of this section, the magnitude of the eddy kinetic energy budget components, for example, is significantly exaggerated. Construction of an improved stratospheric model is currently in progress at the Geophysical Fluid Dynamics Laboratory.

Acknowledgments. The authors are deeply grateful to Mr. J. L. Holloway, Jr., who directed the construction of very extensive computer programs for this model, to Mr. D. G. Hahn who developed a comprehensive system of computer programs for the model analysis and to Mr. D. Daniel who was responsible for the operation of the model code. Special appreciation is extended to Dr. J. Smagorinsky for his efforts to provide a research environment where projects of this scope and magnitude can be undertaken.

Various technical assistance of Messrs. E. J. Green, L. L. Dimmick, S. A. Kenety, P. G. Tunison and Mrs. E. Thompson was indispensable in the preparation of the manuscript. Drs. Y. Hayashi, K. Miyakoda, D. L. Hartmann and A. H. Oort contributed valuable comments on the manuscript and a number of stimulating discussions.

REFERENCES

Adler, R. F., 1973: Mean meridional circulation in the Southern Hemisphere stratosphere during the polar night. Atmos. Sci. Pap. No. 209, Colorado State University, 25 pp. [NTIS N74-17112/5GI].

Byron-Scott, R., 1967: A stratospheric general circulation experiment incorporating diabatic heating and ozone photochemistry. *Publ. Meteor.*, No. 87, McGill University, 201 pp.

Charney, J. G., 1969: A further note on large-scale motions in the tropics. *J. Atmos. Sci.*, **26**, 182–185.

——, and P. G. Drazin, 1961: Propagation of planetary-scale disturbances from the lower into the upper atmosphere. *J. Geophys. Res.*, **66**, 83–109.

Clark, J. H. E., 1970: A quasi-geostrophic model of the winter stratospheric circulation. *Mon. Wea. Rev.*, **98**, 443–461.

Crutcher, H. L., and J. M. Meserve, 1970: Selected level heights, temperatures and dew points for the Northern Hemisphere. NAVAIR 50-1C-52, Naval Weather Service Command [Govt. Printing Office].

Cunnold, D., F. Alyea, N. Phillips and R. Prinn, 1975: A three-dimensional dynamical-chemical model of atmospheric ozone. *J. Atmos. Sci.*, **32**, 170–194.

Dickinson, R. E., 1969: Theory of planetary wave-zonal flow interaction. *J. Atmos. Sci.*, **26**, 73–81.

——, 1971: Analytical model for zonal wind in the tropics: I. Details of the model and simulation of gross features of the zonal mean troposphere. II. Variation of the tropospheric mean structure with season and differences between hemispheres. *Mon. Wea. Rev.*, **99**, 501–523.

Dopplik, T. G. 1971: The energetics of the lower stratosphere including radiative effects. *Quart. J. Roy. Meteor., Soc.*, **97**, 209–237.

Eliassen, A., and E. Palm, 1960: On the transfer of energy in stationary mountain waves. *Geophys. Publ.*, **22**, 1–23.

Fritz, S., 1974: On the cause of the annual and semi-annual variation of radiance (or temperature) from the tropical stratosphere. *J. Atmos. Sci.*, **31**, 813–822.

Hahn, D. G., and S. Manabe, 1975: The role of mountains in the South Asian monsoon circulation. *J. Atmos. Sci.*, **32**, 1515–1541.

Hartmann, D. L., 1975: The structure and dynamics of the Southern Hemisphere stratosphere during late winter, 1973. Ph.D. thesis, Geophysical Fluid Dynamics Program, Princeton University, 261, pp.

Hayashi, Y., 1974: Spectral analysis of tropical disturbances appearing in a GFDL general circulation model. *J. Atmos. Sci.*, **31**, 180–218.

Hering, W. S., and T. R. Borden, 1964: Ozonesonde observations over North America. Air Force Cambridge Research Laboratories, Environ. Res. Pap. No. 38, Vol. 2, 280 pp. [AFCRL 64-30(II); NTIS AD-604 880].

Holloway, J. L., Jr., and S. Manabe, 1971: Simulation of climate by a global general circulation model: I. Hydrologic cycle and heat balance. *Mon. Wea. Rev.*, **99**, 335–370.

Holton, J. R., 1974: Forcing of mean flows by stationary waves. *J. Atmos. Sci.*, **31**, 942–945.

Hunt, B. G., and S. Manabe, 1968: An investigation of thermal tidal oscillations in the earth's atmosphere using a general circulation model. *Mon. Wea. Rev.*, **96**, 753–766.

Hydrographic Office, U. S. Navy, 1944: *World Atlas of Sea Surface Temperature*, 2nd ed. H. O. Publ. No. 225, with supplements (reprinted 1969) [Available from U. S. Naval Oceanographic Office, Wash., D. C.]

Kasahara, A., and T. Sasamori, 1974: Simulation experiments with a 12-layer stratospheric global circulation model. II. Momentum balance and energetics in the stratosphere. *J. Atmos. Sci.*, **31**, 408–421.

——, —— and W. M. Washington, 1973: Simulation experiments with a 12-layer stratospheric global circulation model. I. Dynamical effect of earth's orography and thermal influence of continentality. *J. Atmos. Sci.*, **30**, 1229–1251.

Krishnamurti, T. N., 1961: The subtropical jet stream of winter. *J. Meteor.*, **18**, 172–191.

Kuo, H.-L., 1956: Forced and free meridional circulation in the atmosphere. *J. Meteor.*, **13**, 561–568.

Kurihara, Y., and J. L. Holloway, Jr., 1967: Numerical integration of a nine-level global primitive equations model formulated by the box method. *Mon. Wea. Rev.*, **95**, 509–530.

Labitzke, K., and H. van Loon, 1972: The stratosphere in the Southern Hemisphere. *Meteorology of the Southern Hemisphere, Meteor. Monogr.*, No. 35, 113–138.

—— *et al.* 1972: Climatology of the stratosphere in the Northern Hemisphere. Part I. Heights, temperatures and geostrophic resultant wind speeds at 100, 50, 30 and 10 mb. *Meteor. Abhand., Inst. Meteor., Berlin*, **100**, No. 4.

Mahlman, J. D., 1969a: Energetics of a "minor breakdown" of the stratospheric polar night vortex. *J. Atmos. Sci.*, **26**, 1306–1317.

——, 1969b: Heat balance and mean meridional circulations in the polar stratosphere during the sudden warming of January 1958. *Mon. Wea. Rev.*, **97**, 534–540.

——, 1973a: Preliminary results from a three-dimensional general-circulation/tracer model. *Proc. Second Conf. Climate Impact Assessment Program*, A. J. Broderick, Ed. [DOT-TSC-OSC-73-4, 321–337].

——, 1973b: On the maintenance of the polar front jet stream. *J. Atmos. Sci.*, **30**, 544–557.

——, and S. Manabe, 1972: Numerical simulation of the stratosphere: Implications for related climatic change problems. *Proc. Survey Conf. Climatic Impact Assessment Program*, A. E. Barrington, Ed. [DOT-TSC-OST-72-13, 186–193].

——, and W. J. Moxim, 1976: A method for calculating more accurate budget analysis of "sigma" coordinate model results. *Mon. Wea. Rev.*, **104**, 1102–1106.

Manabe, S., 1969: Climate and ocean circulation: I. The atmosphere and the hydrology of the earth's surface. *Mon. Wea. Rev.*, **97**, 739–774.

——, and R. F. Strickler, 1964: Thermal equilibrium of the atmosphere with a convective adjustment. *J. Atmos. Sci.*, **21**, 361–385.

——, and R. T. Wetherald, 1967: Thermal equilibrium of the atmosphere with a given distribution of relative humidity. *J. Atmos. Sci.*, **24**, 241–259.

——, and B. G. Hunt, 1968: Experiments with a stratospheric general circulation model. I. Radiative and dynamic aspects. *Mon. Wea. Rev.*, **96**, 477–502.

——, and T. B. Terpstra, 1974: The effects of mountains on the general circulation of the atmosphere as identified by numerical experiments. *J. Atmos. Sci.*, **31**, 3–42.

——, and J. L. Holloway, Jr., 1975: The seasonal variation of the hydrologic cycle as simulated by a global model of the atmosphere. *J. Geophys. Res.*, **80**, 1617–1649.

——, J. Smagorinsky and R. F. Strickler, 1965: Simulated climatology of a general circulation model with a hydrologic cycle. *Mon. Wea. Rev.*, **93**, 769–798.

——, D. G. Hahn and J. L. Holloway, Jr., 1964: The seasonal variation of the tropical circulation as simulated by a global model of the atmosphere. *J. Atmos. Sci.*, **31**, 43–83.

Matsuno, T., 1970: Vertical propagation of stationary planetary waves in the winter Northern Hemisphere. *J. Atmos. Sci.*, **27**, 871–883.

——, 1971: A dynamical model of the stratosphere sudden warming. *J. Atmos. Sci.*, **28**, 1479–1494.

McIntyre, M. E., 1972: Baroclinic instability of an idealized model of the polar night jet. *Quart. J. Roy. Meteor. Soc.*, **98**, 165–174.

Miyakoda, K., 1963: Some characteristic features of winter circulation in the troposphere and the lower stratosphere. Tech. Rep. No. 14, Grant NSF-GP-471, Dept. Geophys. Sci., The University of Chicago, 93 pp. [NTIS PB 174 308].

——, R. F. Strickler and G. D. Hembree, 1970: Numerical simulation of the breakdown of a polar night vortex in the stratosphere. *J. Atmos. Sci.*, **27**, 139–154.

Newell, R. E., D. G. Vincent, T. G. Dopplik, D. Ferruzza and J. W. Kidson, 1969: The energy balance of the global atmosphere. *The Global Circulation of the Atmosphere*, G. A. Corby, Ed., Roy. Meteor. Soc., 42–90.

——, G. F. Hermann, J. W. Fullmer, W. R. Tahnk and M. Tanaka, 1974: Diagnostic studies of the general circulation of the stratosphere. *Proc. Intern. Conf. Structure, Composition, and General Circulation of the Upper and Lower Atmosphere and Possible Anthropogenic Perturbations*, Vol. I, Melbourne, Australia, 17–82 [Published by Office of Secretary, IAMAP].

Oort, A. H., 1964: On the energetics of the mean and eddy circulation in the lower stratosphere. *Tellus*, **16**, 309–327.

——, and E. M. Rasmusson, 1971: Atmospheric Circulation Statistics. NOAA Prof. Pap. No. 5, 323 pp. NOAA, U. S. Dept. of Commerce [NTIS COM-72-50295].

Peng, L., 1965: A simple numerical experiment concerning the general circulation in the lower stratosphere. *Pure Appl. Geophys.*, **61**, 191–218.

Phillips, N. A., 1957: A coordinate system having some special advantages for numerical forecasting. *J. Meteor.*, **14**, 184–185.

Reed, R. J., and C. L. Vleck, 1969: The annual temperature variation in the lower tropical stratosphere. *J. Atmos. Sci.*, **26**, 163–167.

Richards, M. E., 1967: The energy budget of the stratosphere during 1965. Planetary Circulations Project, MIT Rep. No. 21, Contract AT(30-1)2241 [NTIS MIT-2241-38].

Smagorinsky, J., 1963: General circulation experiments with the primitive equations: I. The basic experiment. *Mon. Wea. Rev.*, **91**, 99–164.

——, S. Manabe and J. L. Holloway, Jr., 1965: Numerical results from a nine-level general circulation model of the atmosphere. *Mon. Wea. Rev.*, **93**, 727–768.

Taljaad, J. J., H. van Loon, H. L. Crutcher and R. L. Jenne, 1969: *Climate of the Upper Air.* Vol. I, *Southern Hemisphere.* NAVAIR 50-1C-55 [Available from Naval Weather Service Command, Washington Naval Yard, Building 200, Washington, D. C. 20390].

Trenberth, K. D., 1973: Dynamic coupling of the stratosphere with the troposphere and sudden stratospheric warmings. *Mon. Wea. Rev.*, **101**, 306–322.

van Loon, H., R. L. Jenne and K. Labitzke, 1972: Climatology of the stratosphere in the Northern Hemisphere. Part 2. Geostrophic winds at 100, 50, 30 and 10 mb. *Meteor. Abhand., Inst. Meteor., Berlin*, **100**, No. 5.

White, R. M., 1954: The counter-gradient flux of sensible heat in the lower stratosphere. *Tellus*, **6**, 177–179.